RESEARCH INTO THE SAFETY AND EFFICIENCY OF UNDERGROUND PLACER MINING AND FROZEN GROUND

By
Scott L. Huang

Open File Report 83-3

PO NO. B4620191

RESEARCH INTO THE SAFETY AND EFFICIENCY OF UNDERGROUND PLACER MINING AND FROZEN GROUND

FINAL REPORT

(April 1, 1982 - June 30, 1983)

By

Scott L. Huang

Report on

Contract No. B4620191
Fairbanks Office
U.S. Bureau of Mines
Department of the Interior

September, 1983

ABSTRACT

Some of the underground excavation problems encountered in arctic and subarctic environments associated with thermal disturbance are excessive settlement of ground surface and pronounced displacement around openings.

This study investigated the possible links between the significant settlement. Ground temperature was found to be the most influential. An empirical equation was developed for the USBM gravel room to predict the effect of temperature on creep of frozen gravel. Separation of the roof gravel and silt was observed as steady heating process increased the gravel temperature by one degree.

The temperature dependent material constants were estimated from the laboratory testings. The factors affecting the creep characteristics were temperature and applied stress level. The primary creep behavior of frozen gravel loaded under 18% of unconfined compressive strength at 25° and 29°F could be predicted empirically.

ACKNOWLEDGEMENT

This study was supported by the U.S. Bureau of Mines, Fairbanks Office, Fairbanks, Alaska 99701 under Contract No. B4620141. Travel to the tunnel site during this study was supported by the Office of Surface Mining, Division of Technical Services and Research, Washington, D.C. 20240, under Contract No. G1125151.

The research reported herein was performed by Scott L. Huang. Field monitoring and laboratory testing were conducted by Mr. Harold Garbeil, graduate student of geological engineering, as part of the fulfillment of requirements for a M.S. degree.

TABLE OF CONTENTS

TABLE OF CONTENTS (cont')

LIST OF FIGURES

LIST OF FIGURES (cont')

LIST OF TABLES

INTRODUCTION

Increased demand for resources of all types will necessitate further mining activities in arctic and subarctic environments. Because of the high frequency of encountering frozen ground in these regions, construction of a structure in the areas is often a challenging task. Underground structures in frozen ground have pronounced creep deformation resulting from disturbance of thermal equilibrium of the surrounding materials. For projects concerned with safety of miners and cost of operation, the uncertainties in achieving the final goals are high unless certain information is well understood. It is for this reason that the research was conducted to identify a proper method which improves underground design and construction in permafrost regions.

In the design of an underground placer mine in arctic and subarctic environments, the engineer has to perform the following tasks:

- to understand the geological condition in which the excavation will be made;
- to understand and to predict the response of the natural frozen materials to the change of environments imposed by excavation, construction, and various types of activities; and
- to modify, if necessary and possible, the behavior of frozen ground in order to ensure adequate performance of the structure.

These three tasks can be accomplished by means of geological investigation and engineering analysis and design.

In order to obtain the necessary geological and engineering data for a practical underground mine design in the northern region, the

U.S. Army Cold Region Research and Engineering Laboratory (USA CRREL) permafrost tunnel was used. The USA CRREL permafrost tunnel offers an unique opportunity for monitoring and investigating the behavior of frozen ground. The local geology and material properties of the tunnel have been described by Sellmann (1967 and 1972), Thompson and Sayles (1972), and Pettibone and Waddell (1969). Work accomplished by those investigators provided this research with a better understanding of the tunnel complex, and therefore, the study could be focused upon the more significant factors. Parameters such as material type, ground temperature, thickness of overburden, and opening geometry were thought to be crucial to the response.

One of the major objectives of this study was to establish the long term convergence rates of different frozen materials. In addition, the measured creep rates were compared with the contributing factors to find the possible relationships. The second prime objective was to study the temperature effects on the creep responses of frozen materials. Thermal influence on ground stability is, by far, the most worrisome problem encountered in arctic engineering design. In this research, the temperature effect was isolated and quantified through field and laboratory studies. The third objective was to investigate the possible parting in the materials overlying the opening. Strata separation was first observed by Pettibone and Waddell (1969) immediately after tunnel excavation. It is likely to occur again under certain conditions. Identification of the critical condition is the very reason which makes this research more meaningful.

USA CRREL PERMAFROST TUNNEL

History

The USA CRREL tunnel is located approximately 12 miles north of Fairbanks in the town of Fox, Alaska (Figure 1). In 1963, the tunnel was cut into a near-vertical silt escarpment formed by old placer mining operations. During the following three winters the tunnel was excavated through frozen silt of late Quaternary age for the entire 360 ft. A vertical shaft 45 ft. deep and 4 ft. in diameter was augered in 1966 for ventilation. In the winter of 1968-1969, the Bureau of Mines dug a winze (approx. 100 ft. from the portal) from the existing tunnel through the placer-gold bearing frozen gravel into bedrock (Figure 2). During the same period of time, three rooms were also excavated in the gravel deposit which overlies bedrock. The openings are accessible and have been well maintained in a frozen state since excavation. The materials and types of ground ice are common to many permafrost areas, and provide a very useful site for investigating the engineering properties of perennially frozen soils.

Tunnel Geology

The geology and material properties of the tunnel are described in great detail by Sellmann (1967 and 1972). This paper only summarizes the geological studies conducted by USA CRREL in the tunnel. An idealized geological cross-section of the tunnel was cited from Sellmann's 1967 report (Figure 3) to illustrate the sedimentary formations in the area.

Silt. Silt is the dominant constituent of the late Pleistocene deposits in the area. The silt sections are as much as 55 ft. thick.

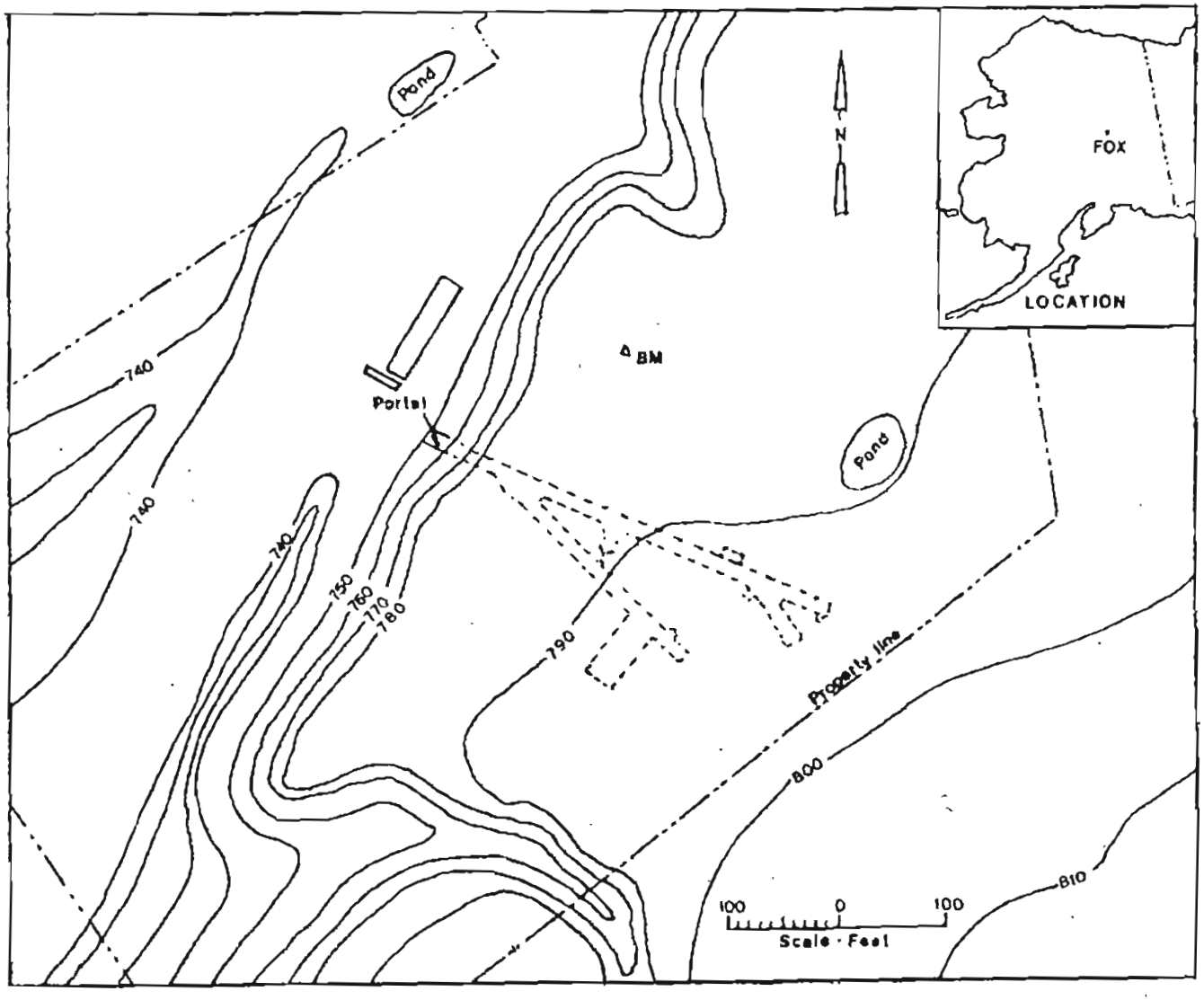

Figure 1. Topographic map of the USA CRREL permafrost tunnel at Fox, Alaska.

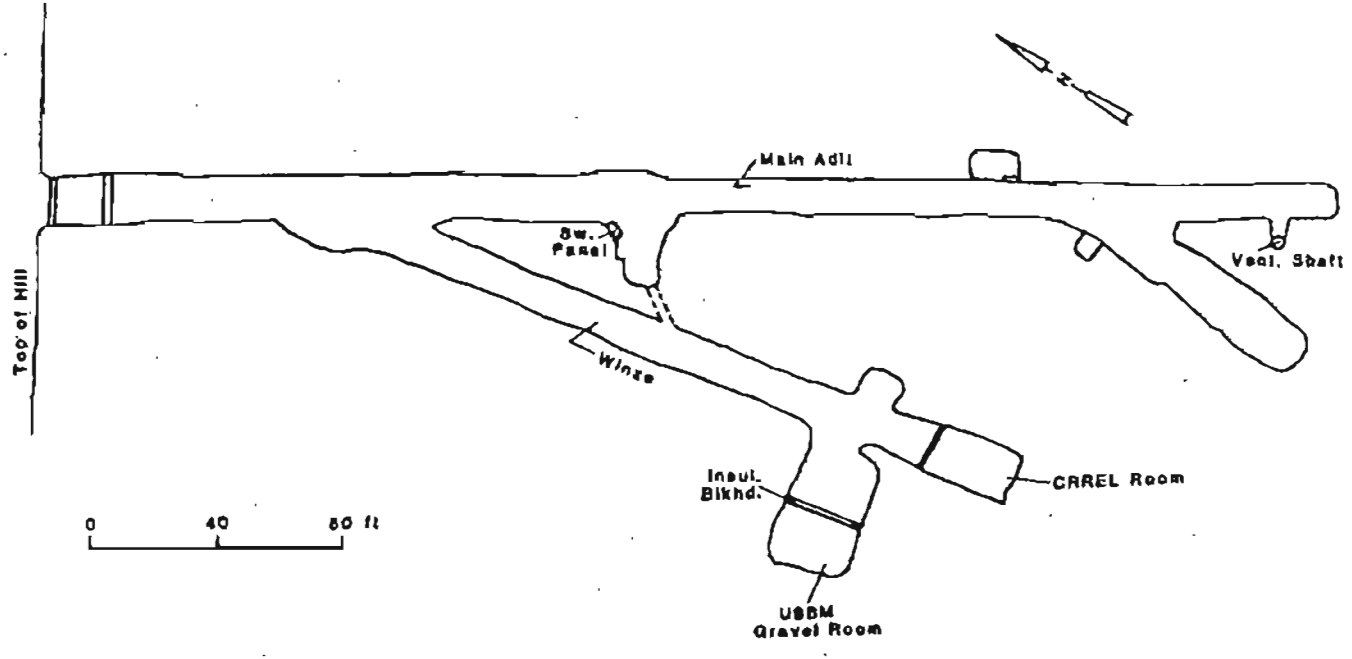

Figure 2. USA CRREL permafrost tunnel plan map.

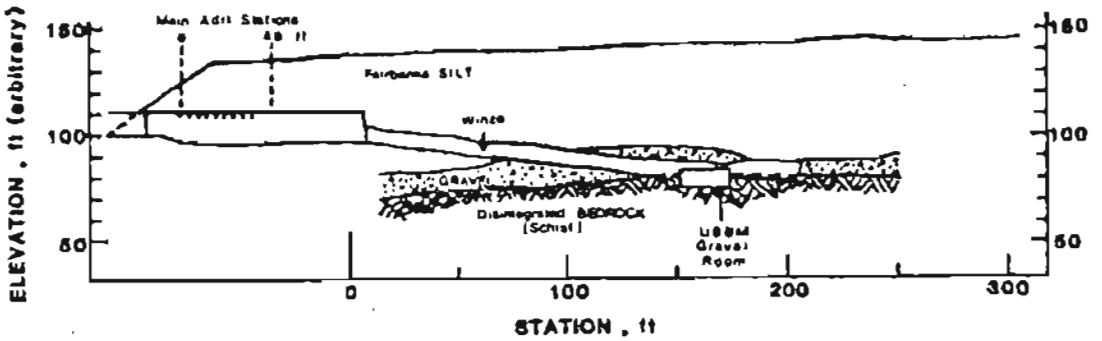

Figure 3. USA CRREL permafrost tunnel section showing site geology (Sellmann, 1967).

The analysis of silt samples from the tunnel section indicated that 68% of the material is within the silt size range and the uniformity coefficient is about 3.8. The index indicates that silt material is fairly uniform in size. The bulk density of the silt ranges between 78 and 115 pcf and averaged 92 pcf, with moisture contents between 32 and 139% by dry weight. The dry density ranges from 33 to 87 pcf with an average of 54 pcf. The silt exposures in the tunnel contain massive ice-wedges and small ice-lenses. The large volume of ground ice, 53 to 80% by volume, generates unusual engineering problems. The silt strength is influenced largely by its high ice volume.

Gravel. The early Wisconsin gravels were stream deposited with imbrication of the pebbles, cobbles and sands. Sand and silt lenses of Illinoian age are common in the upper part of the stratified gravel. The average thickness of the gold-bearing gravel in the vicinity of the tunnel is around 13 ft. Moisture contents of the gravel range from 8.9 to 10.3% by dry weight. Particle size analysis showed that 55% of the deposit is in the gravel range. The uniformity coefficient is around 4.5 which indicates that the gravel deposit is not well sorted. Although the gravel, similar to the silt, is bonded with ice, it does not contain massive ground ice. The absence of ice wedges or ice lenses in the gravel deposit, in addition to its greater mechanical strength, make the formation much more stable than the silt formation. Ice is visible in the voids, but the gravel appears to retain particle-to-particle contact.

The 30 by 70 foot USBM gravel room has a floor of bedrock. The walls and roof consist of coarse conglomerate. The gravel extends

approximately 6 feet into the roof. The remaining overburden is silt of 50 - 65 feet in thickness.

Bedrock. The bedrock in the area is Birch Creek schist of Precambrian age. It is a gray to brownish graphite-quartz-calcite schist or quartz-mica schist. The bedrock is overlain by frozen gravel. The gravel-bedrock contact is very irregular. The top surface of the bedrock is highly altered and forms a clay layer. Moisture contents of the decomposed bedrock range from 6.5 to 19.9% by dry weight and average 11.7%. Placer gold usually occurs at the contact zone.

Ground Ice. The types of ground ice in the tunnel can be divided into two groups: 1) the small lenses formed by ice segregation, and 2) the massive ice wedges and ice lenses. There are several areas along the tunnel exposure in which massive ground ice is present.

FIELD INSTRUMENTATION AND MONITORING

Instrumentation

Instruments were installed in the USBM gravel room to measure vertical and horizontal movements in response to thermal effects, to investigate the possibility of strata separation between roof gravel and silt, and to record the air and ground temperatures at each station.

The gravel room consisted of 5 vertical convergence stations, 5 thermistor strings, and two multiple-point borehole extensometers (Figure 4). There were also 3 vertical convergence stations and two sets of thermistor strings installed outside the gravel room to record the possible creep behavior changes due to temperature difference.

Tape extensometer points were anchored in the walls, roof and floor (Figure 5). The floor closure point was placed to a depth of 1.5 feet and grouted with a layer of frozen slurry to ensure the stability of the point. A thin water mist was sprayed on each closure point periodically to reduce sublimation of bonding ice. Sublimation transfers ground ice directly from the solid phase into a vapor. By this process the strength of frozen soil greatly reduces. A constant supply of water in the surrounding area of each closure point can dramatically reduce the sublimation of the interstitial ice.

Air temperatures inside the gravel room were recorded continuously with a hygrothermograph (+ 0.2°F accuracy). In addition, the relative humidity of the air was also monitored by the same instrument.

Frozen soil temperatures at each monitoring station were measured with thermistors installed in a borehole. Figure 6 shows a typical

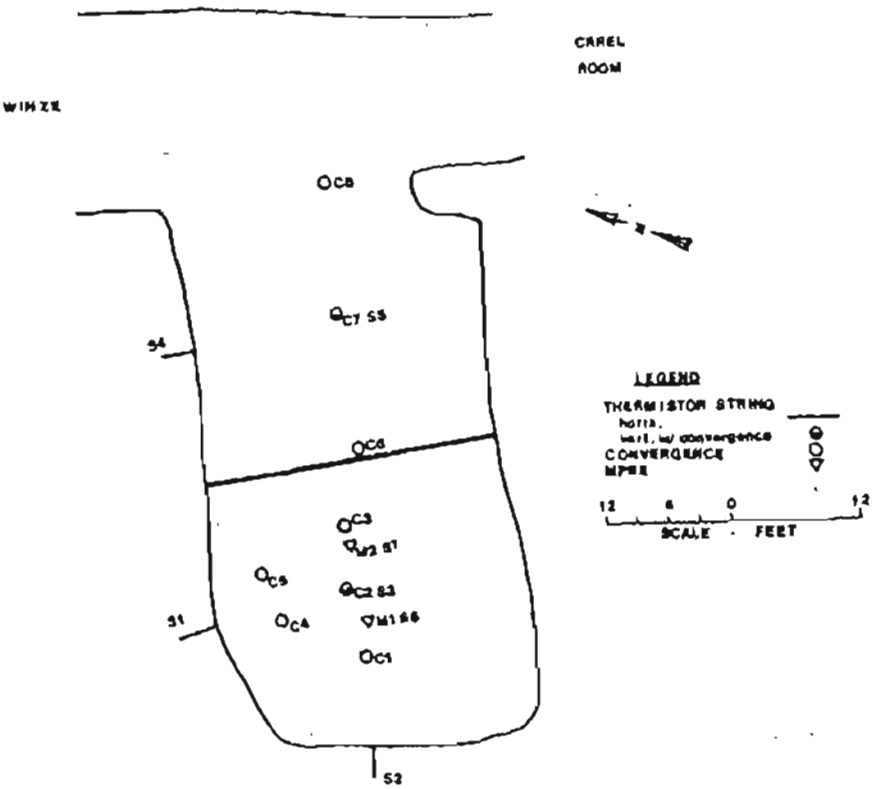

Figure 4. Instrumentation layout in the USBM gravel room.

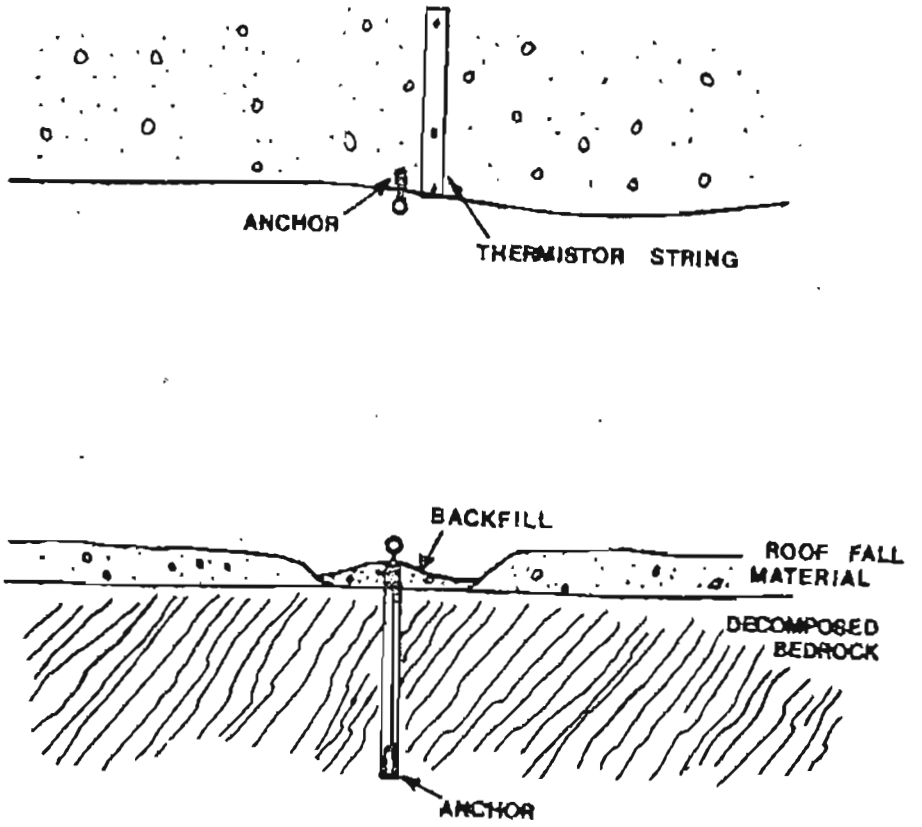

Figure 5. Diagram showing installation of convergence station.

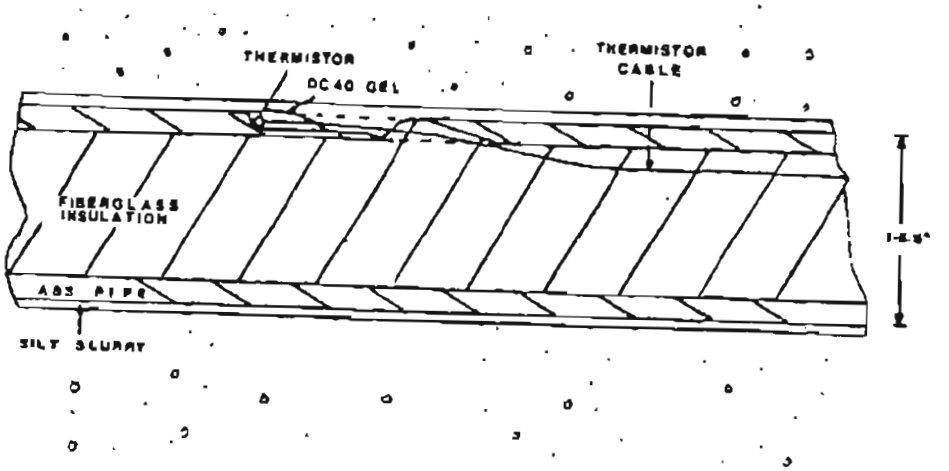

Figure 6. Cross section view of thermistor string.

thermistor string installation. A thermistor (Omega 4400) calibrated to an accuracy of + 0.1°F was mounted to a 1.25 inside diameter ABS pipe. A groove was cut in the pipe so that the thermistor was flush with pipe surface for protection during insertion into the borehole. Each string consisted of several thermistors ranging from two to seven pieces. Inside the pipe, fiberglass insulation was applied to reduce thermal leakage. A thin layer of frozen silt slurry was utilized to grout the thermistor string, providing a continuity between thermistor and the surrounding frozen material. In addition, high thermal conductivity gel (DC 40) was applied around the thermistor to ensure better contact with the borehole. Resistivity changes of the thermistor at each point was measured by a portable resistivity meter with sensitivity of ± 0.1°F.

Roof separation was monitored with two rod-type multiple position borehole extensometers (M1 and M2) manufactured by Irad Gage Co. The M1 station (Figure 7) consisted of 4 C-anchors at 2.5, 5.5, 6.5 and 7.5 ft. position, and the four anchors of M2 station were located at 2.0, 5.0, 6.0 and 9 ft. position. Both borehole extensometers were installed in 2.5 in. diameter holes. The M1 extensometer was installed vertically, and the M2 extensometer was placed 20° to the vertical. The relative movements of anchors with respect to the head were carefully measured with a depth micrometer (Figure 8). The data provided information concerning the parting.

Monitoring

Air Temperature. The ambient temperature of the tunnel varied with the location of monitoring station and with the various types of activities inside the tunnel.

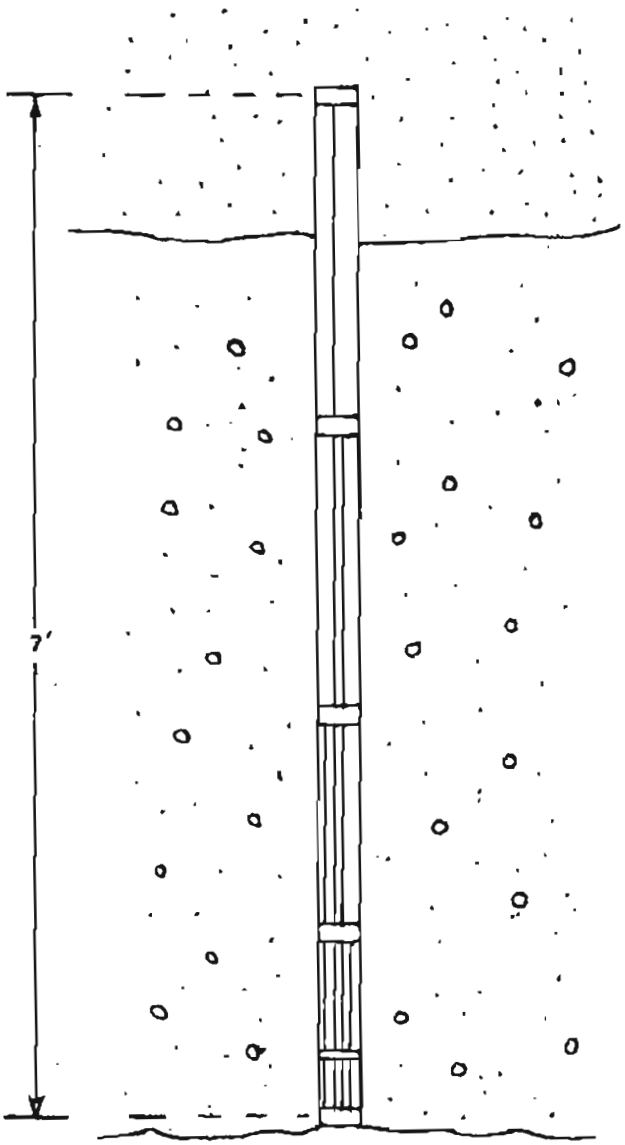

Figure 7. Installation of multiple position borehole extensometer in roof.

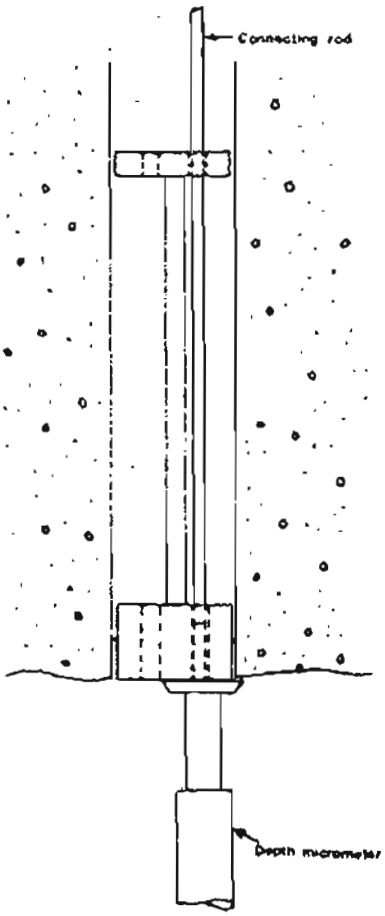

Figure 8. Close-up of instrument head of MPBX and depth micrometer.

The air temperature inside the gravel room was controlled manually by means of a heating element (150W light bulbs) and a ventilation fan. In order to maintain both the opening and the surrounding frozen materials near their ambient temperatures, an insulated bulkhead at the USBM gravel room was constructed.

In the first stage of the study, the insulated bulkhead was removed and cold air was ventilated through a duct from outside to ensure a wider range of working temperatures. Later, this bulkhead was positioned during the heating stage which started April 24, 1983 and ended July 27, 1983.

Figures 9 through 18 and Appendix A summarize air and ground temperatures at stations S1 to S7. Stations S1. S2. S3, S6 and S7 were located in the USBM gravel room, and stations S4 and S5 were at the other side of the bulkhead. The string S1 and S2 were installed in the sidewall and in the face at depths of 4 ft. and 2.5 ft. respectively. String S3 was placed in the roof at a depth of 3.0 ft. Thermistors of strings 6 and 7 were attached to the anchors of M1 and M2. Station S4 and S5 were installed in the outer compartment of the USBM gravel room. String S4 had two thermistors at depths of 1.0 and 2.0 ft. String S5 had three thermistors located with 1.5 ft. interval each.

The curves TH100, TH203, TH300, TH600 and TH700 on Figures 9, 11, 12, 15 and 17 represent the gravel surface temperature variations starting from January 10, 1983 to July 27, 1983. Comparing the curve TH500 with other surface temperatures, the fairly constant temperature distribution of station S5 during the heating stage indicates that

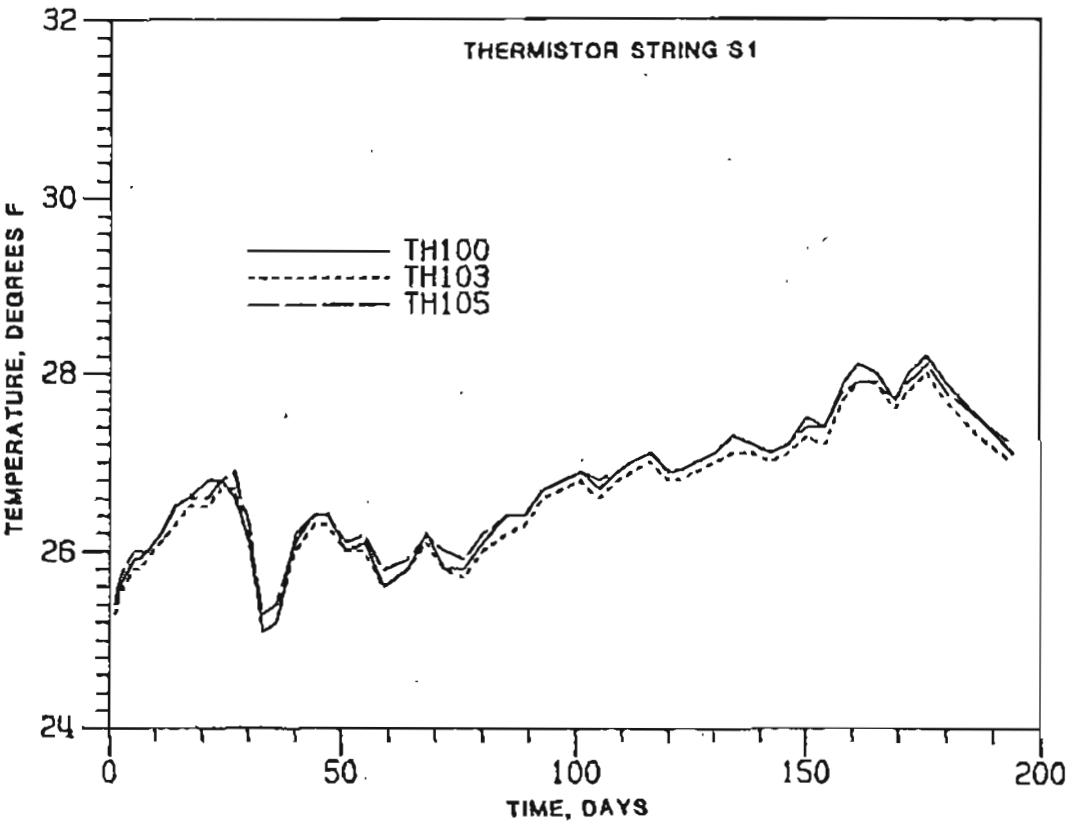

Figure 9. Frozen gravel temperature variations at station S1. (Thermistor location: 0.0, 0.25 and 0.5 ft.)

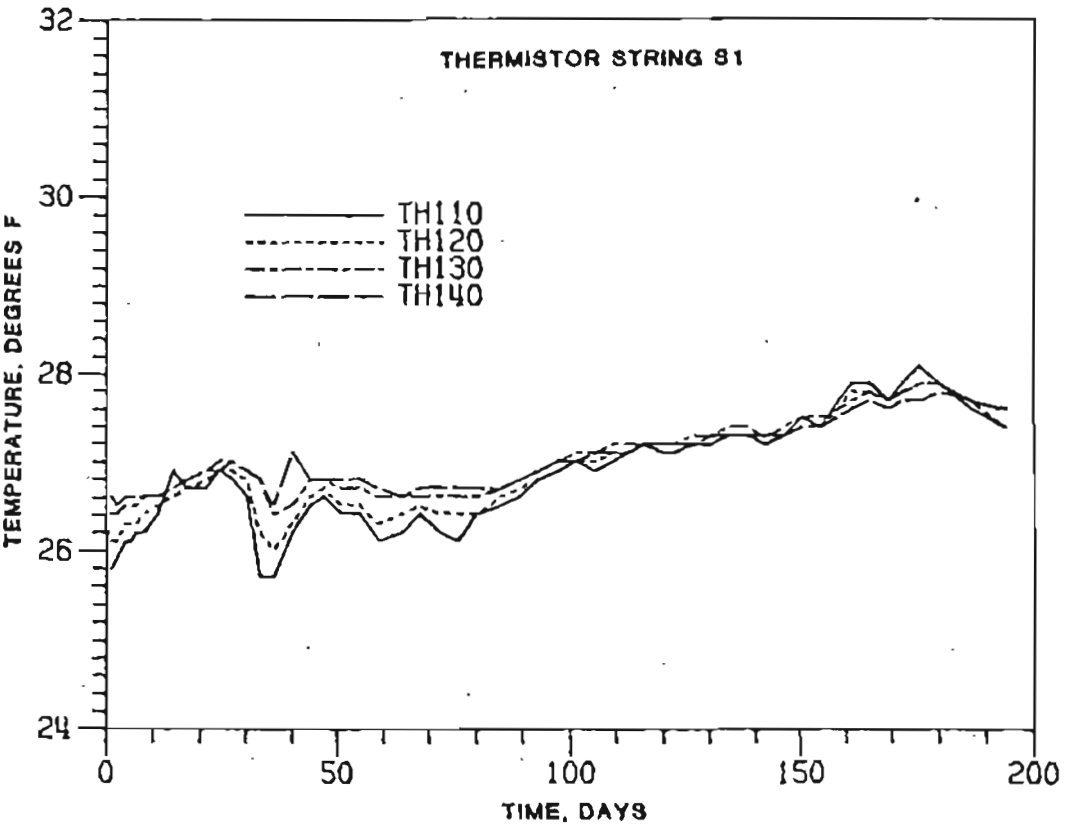

Figure 10. Frozen gravel temperature variations at station S1. (Thermistor location: 1.0, 2.0, 3.0 and 4.0 ft.).

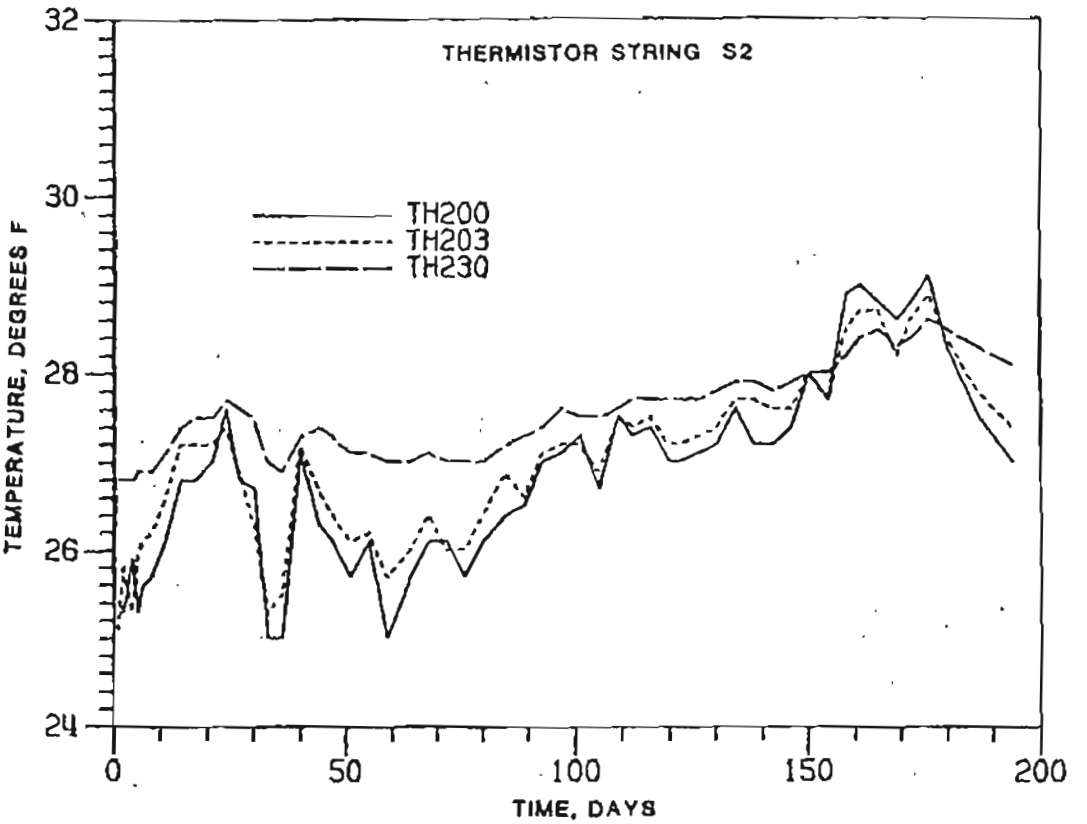

Figure 11. Frozen gravel temperature variations at station S2. (Thermistor locations: -0.5, 0.0 and 2.5 ft.).

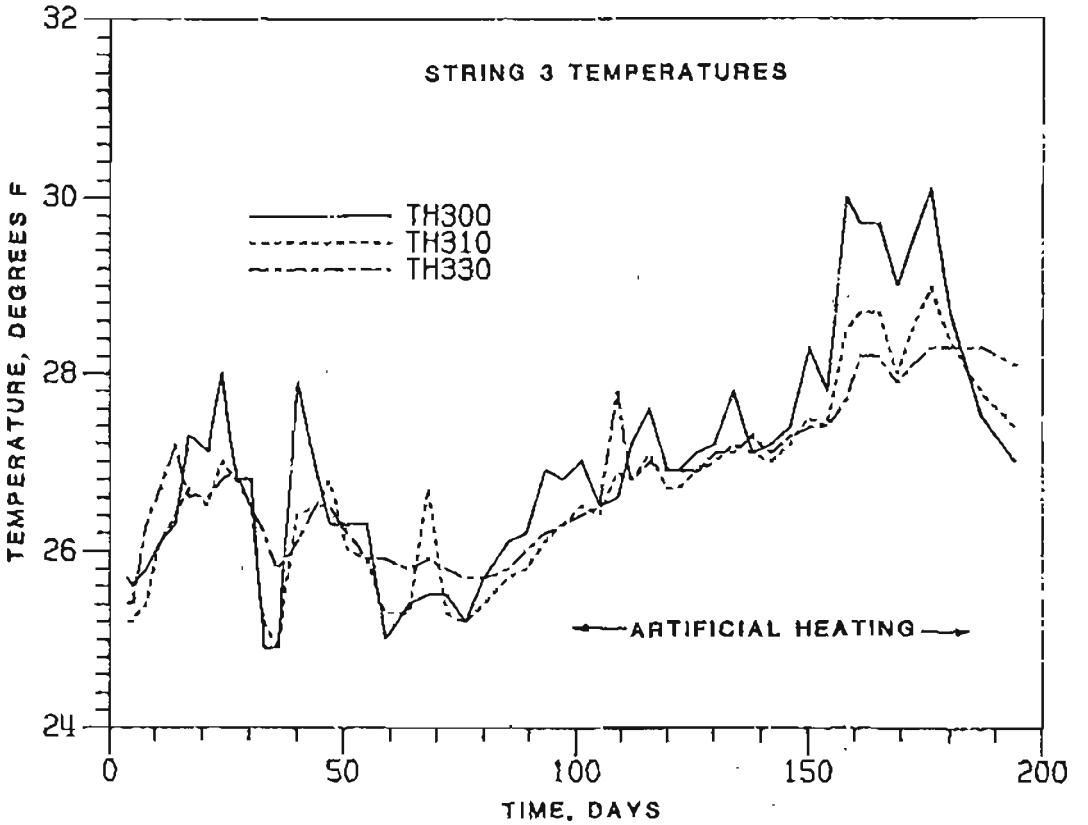

Figure 12. Frozen gravel temperature variations at station S3. (Thermistor location: 0.0, 1.0 and 3.0 ft.).

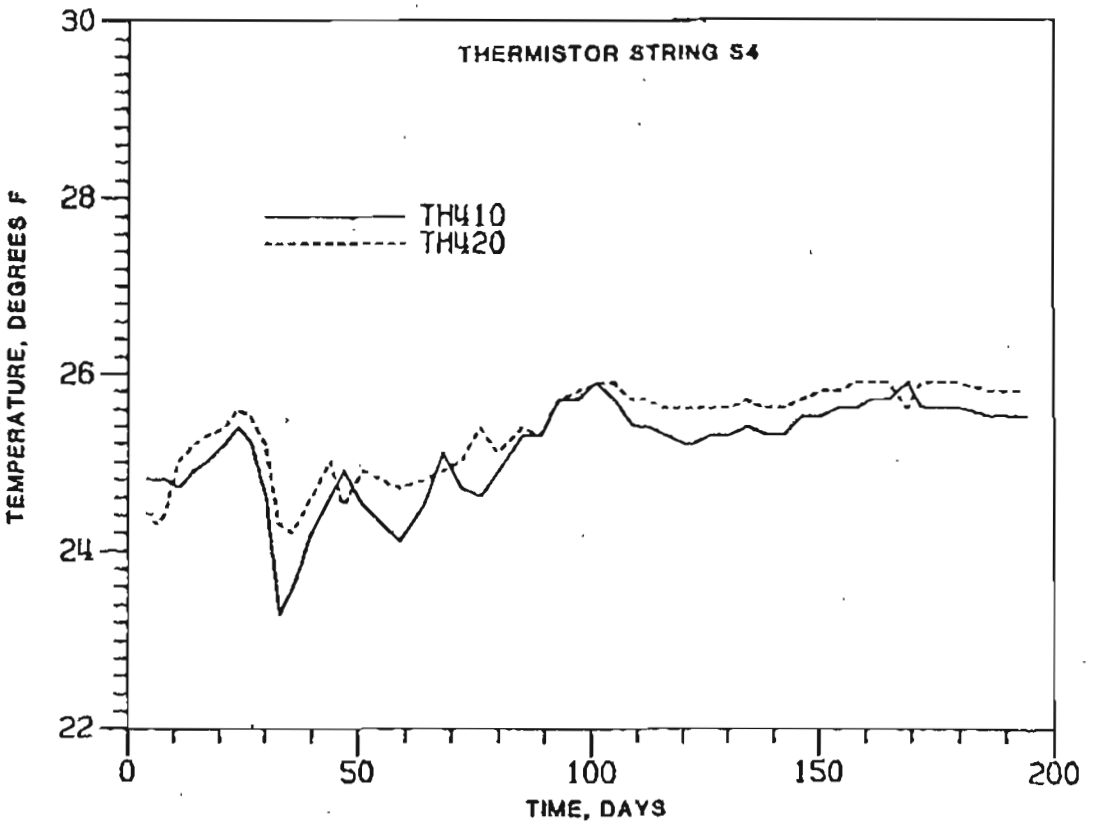

Figure 13. Frozen gravel temperature variations at station S4. (Thermistor location: 1.0 and 2.0 ft.).

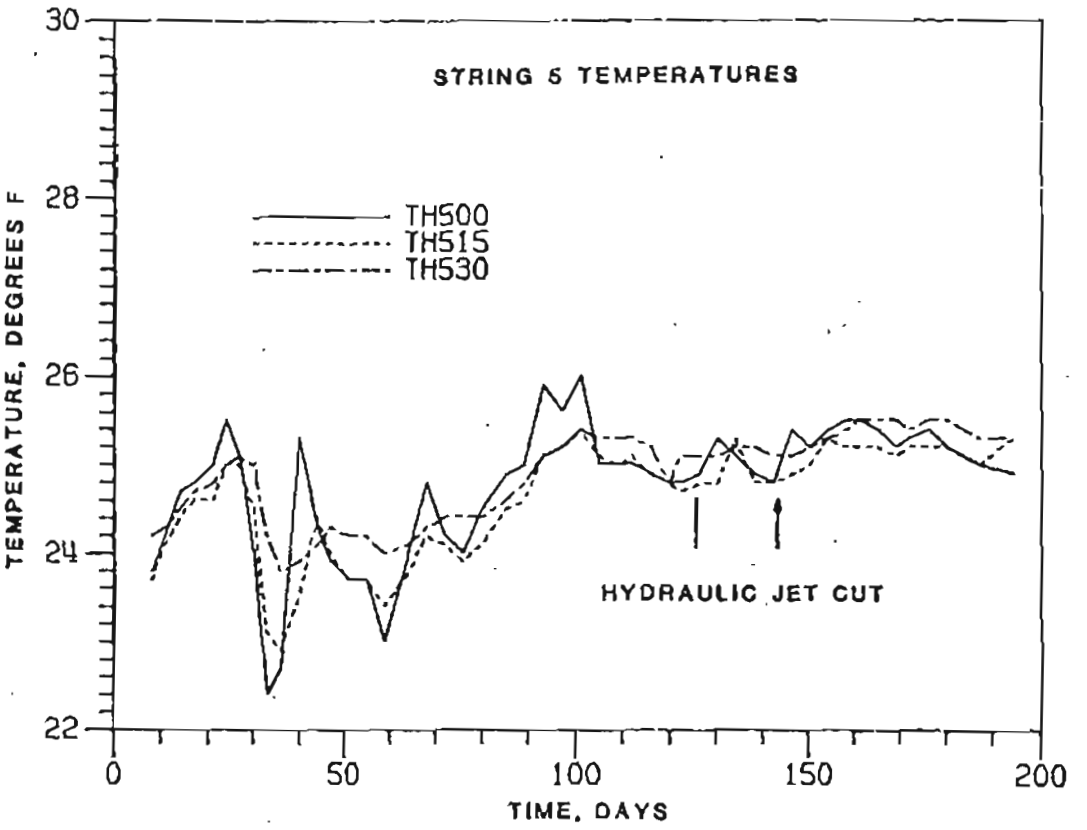

Figure 14. Frozen gravel temperature variations at station S5. (Thermistor location: 0.0, 1.5 and 3.0 ft.).

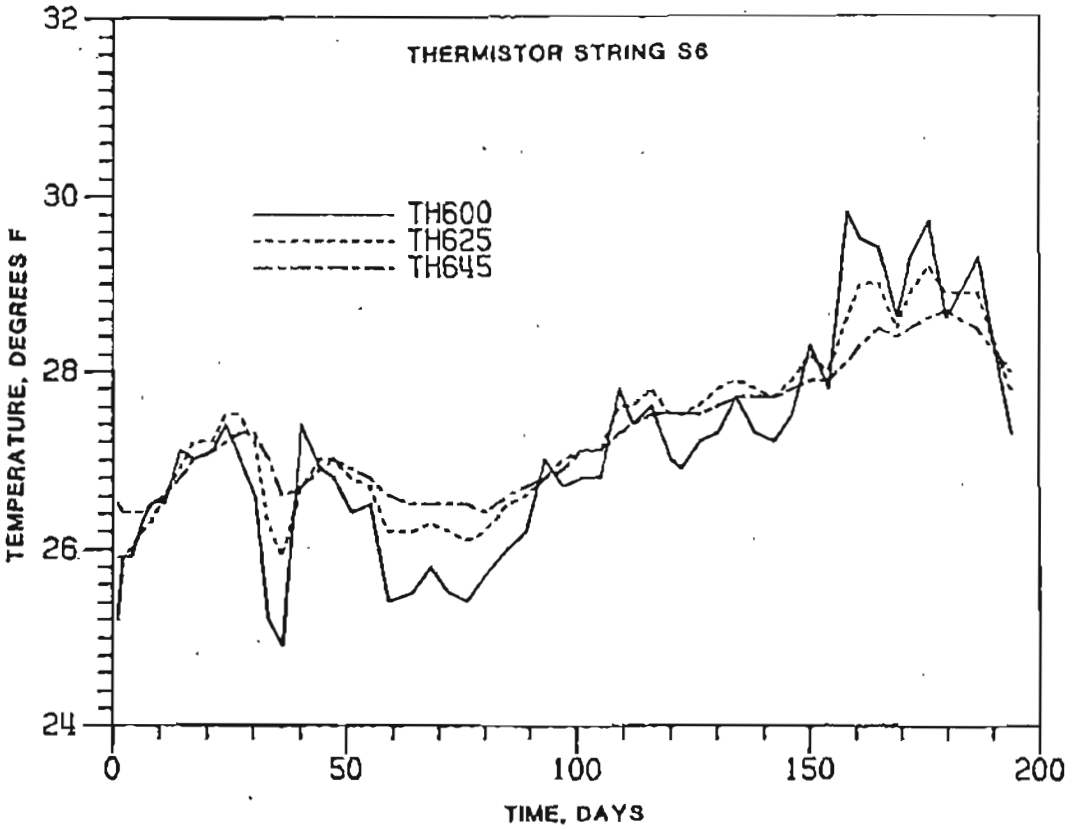

Figure 15. Frozen gravel temperature variations at station S6. (Thermistor location: 0.0, 2.5 and 4.5 ft.).

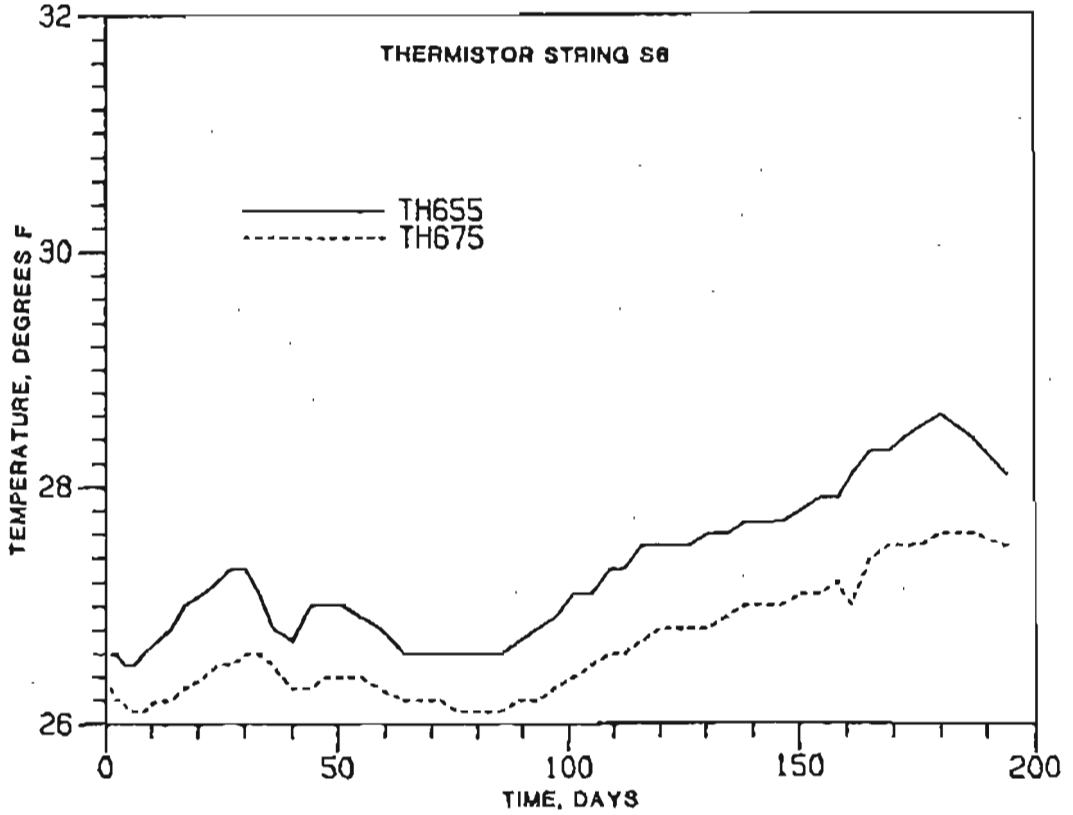

Figure 16. Frozen gravel temperature variations at station S6. (Thermistor location: 5.5 and 7.5 ft.).

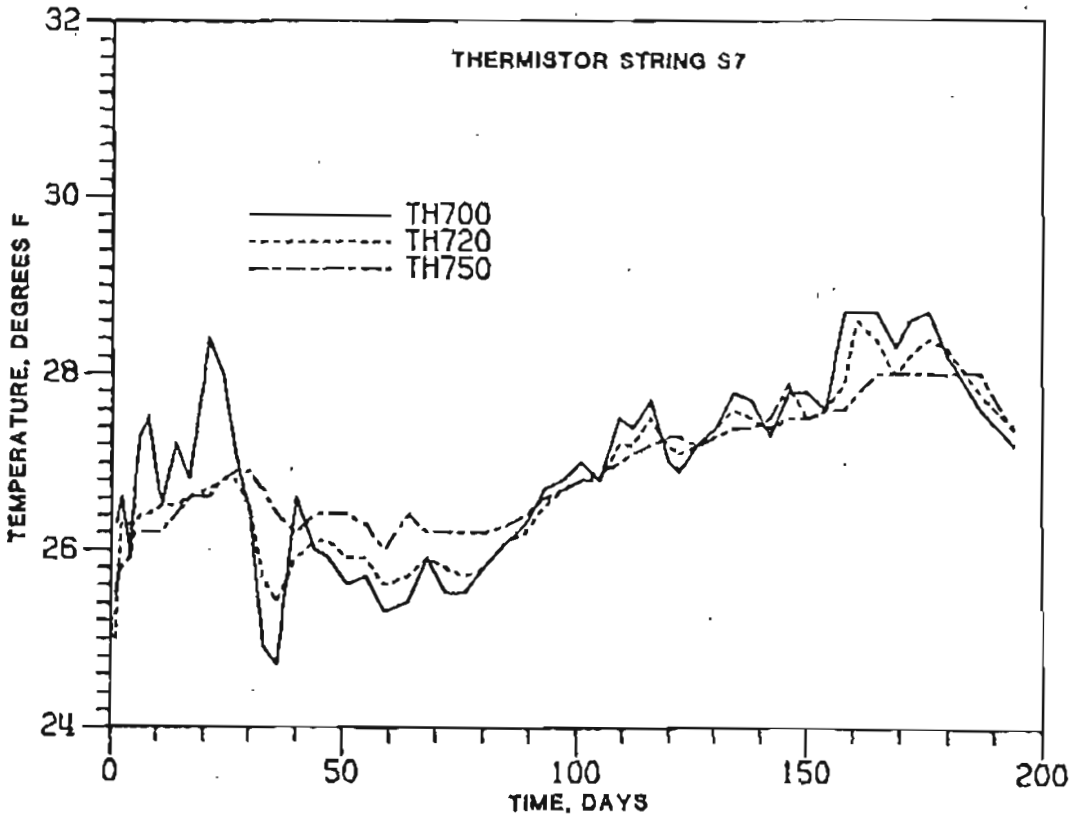

Figure 17. Frozen gravel temperature variations at station S7. (Thermistor location: 0.0, 2.0 and 5.0 ft.).

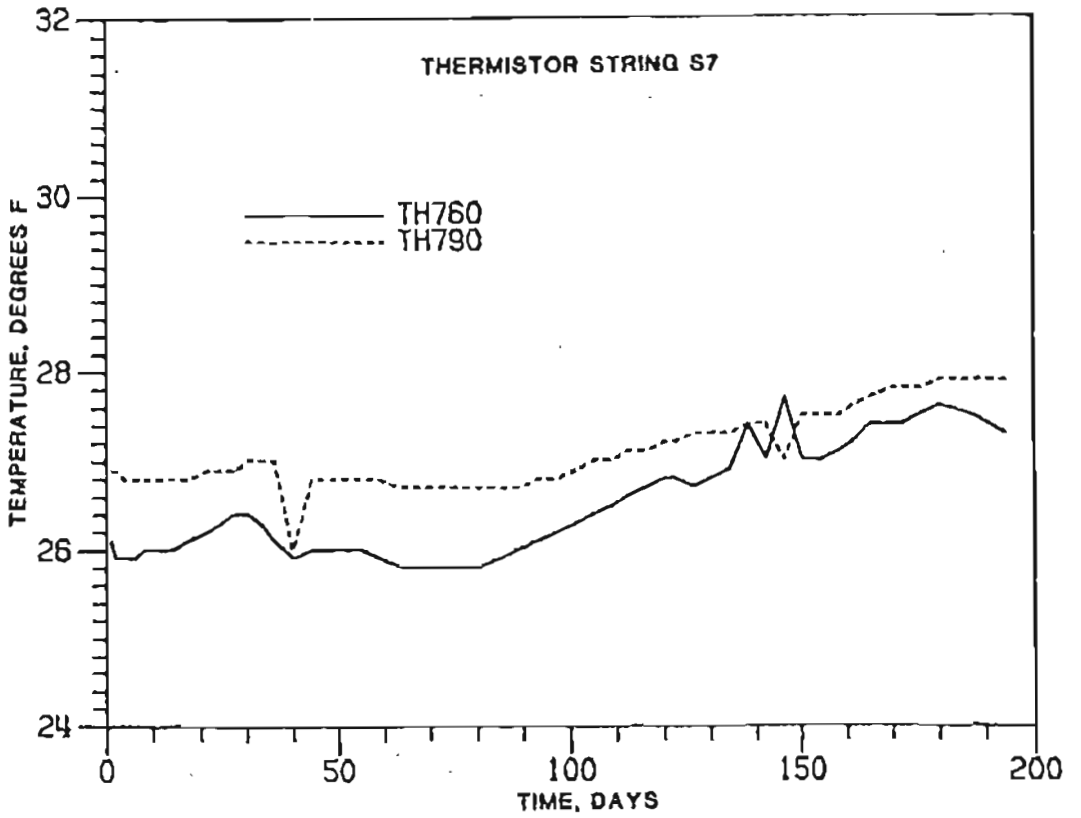

Figure 18. Frozen gravel temperature variations at station S7. (Thermistor location: 6.0 and 9.0 ft.).

heat loss from the gravel room through the insulated bulkhead was very small.

A slight increase of temperature at station S5 was noticed after two hydraulic jet cuttings. There were two cuttings conducted to evaluate the performance of the water jet. The first test was made on May 24, 1983. The second cutting was tested on June 23, 1983, All 400 gallons of water used during both cuttings were pumped from the sump and sprayed on the floor of the winze and outside compartment of the USBM gravel room. Release of latent heat during the phase changes of water to ice increased temperature by 0.6 degrees. The air temperature jumped from its background temperature (24.8°F) to approximately 25.4°F.

Due to a warm winter, the coldest air temperature in the gravel room was around 25°F, much higher than expected. Nevertheless, the heating process began immediately after the refrigeration system was turned on. The gravel room warmed up gradually to a temperature which was thought to be too dangerous to work with, requiring the heating source to be disconnected. The peak temperature in the gravel room was 30.1°F which was at the station S3 (Figure 12).

Air temperature near the floor of the USBM room was monitored by a hygrothermograph (Bendix Model 594) during the first 62 days of study. The temperature variation was plotted and shown in Figure 19. Compared with the air temperature variations at stations S1 through S3, these three curves showed very similar patterns. However, the average air temperature near the floor was about two to three degrees lower than that recorded close to the roof. The lowest temperature recorded by the hygrothermograph was 19°F. This cold period was also

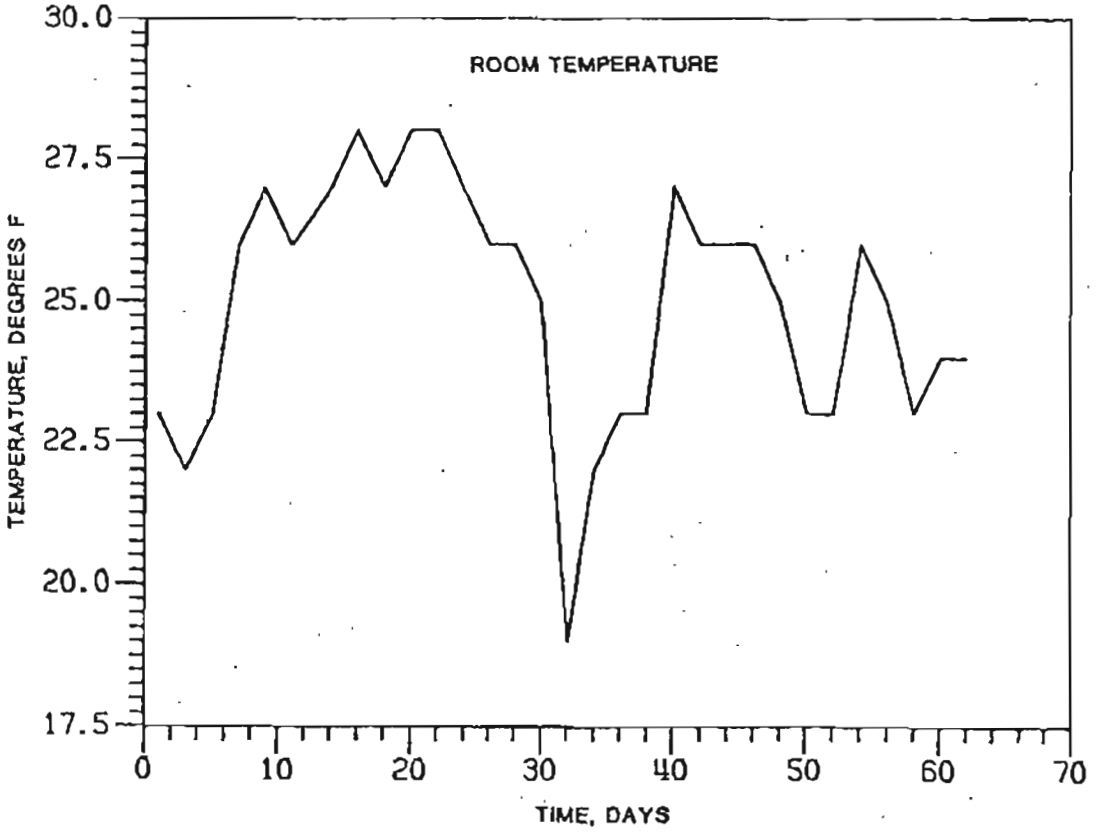

Figure 19. Air temperature distribution near the gravel floor.

monitored by the other stations. Nevertheless, the temperatures at the other stations were not as low as that near the gravel floor.

Relative humidity of the air inside the gravel room was recorded continuously by the same hygrothermograph. Figure 20 indicates the relative humidity changes of the gravel room during the first 62 days. Variation of air humidity depended on the changes of air temperature. The relative humidity ranged from 79% to 59%.

Ground Temperature. Temperatures of frozen soils in the USBM gravel room were recorded with a series of thermistors. Summary plots of the thermistor data at seven ground temperature monitoring stations are shown in Figures 9 through 18. Also, the Appendix A lists the ground temperature information. Figures 9 and 10 show the temperatures of the gravel wall at the surface and at depths of 0.3, 0.5, 1.0, 2.0, 3.0 and 4.0 feet.

By comparison of those temperatures close to the surface (TH103 and TH105) and those at greater depth (TH130 and TH140), it was noticed that the fluctuation of temperature was relatively small for thermistors TH130 and TH140.

The gravel temperature distributions in January, March and June at station S1 were plotted. The diagram (Figure 21) shows that a possible thermal transition zone existed somewhere at a depth of 1 foot from wall surface. Frozen gravel at shallow depths (less than 1 foot) had a thermal gradient ranging from 0.2 to 0.37°F/ft. during January and from 0.54 to 0.64°F/ft. in March. Beyond this transition zone the gradient decreased to a range of 0.07 to 0.18°F/ft. in both months. This information suggests that the short term climatic ef-

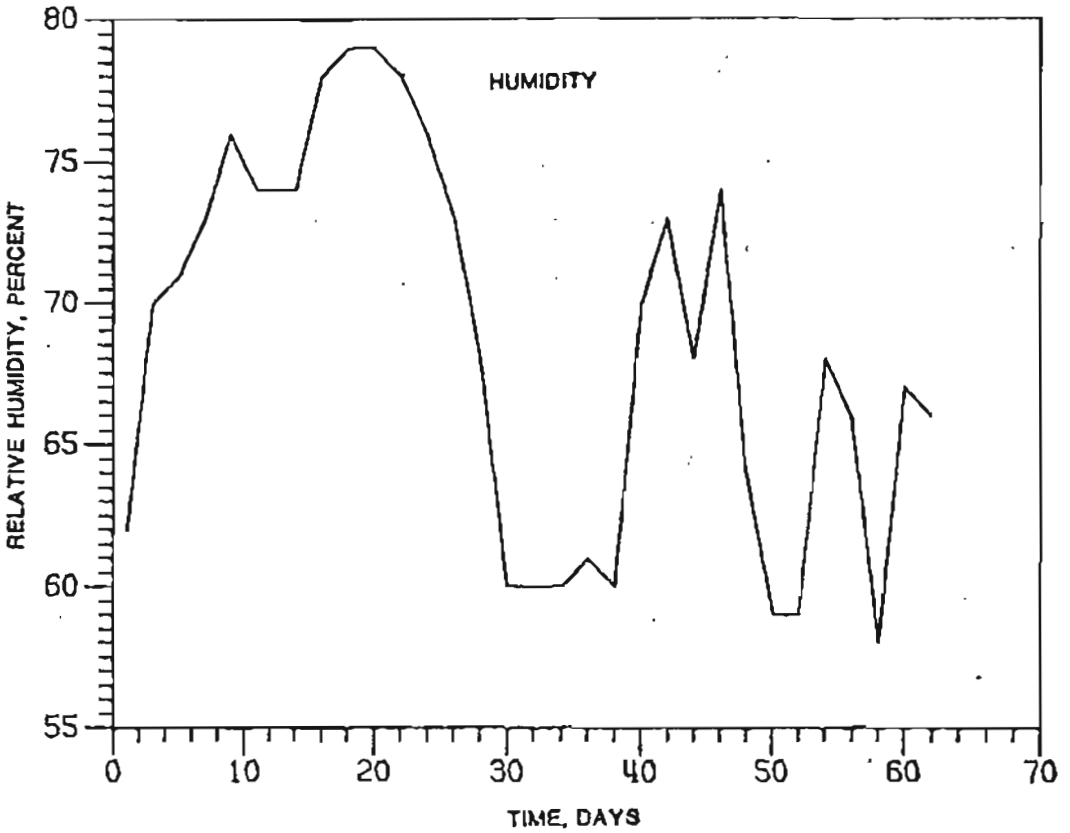

Figure 20. Relative humidity changes of gravel room.

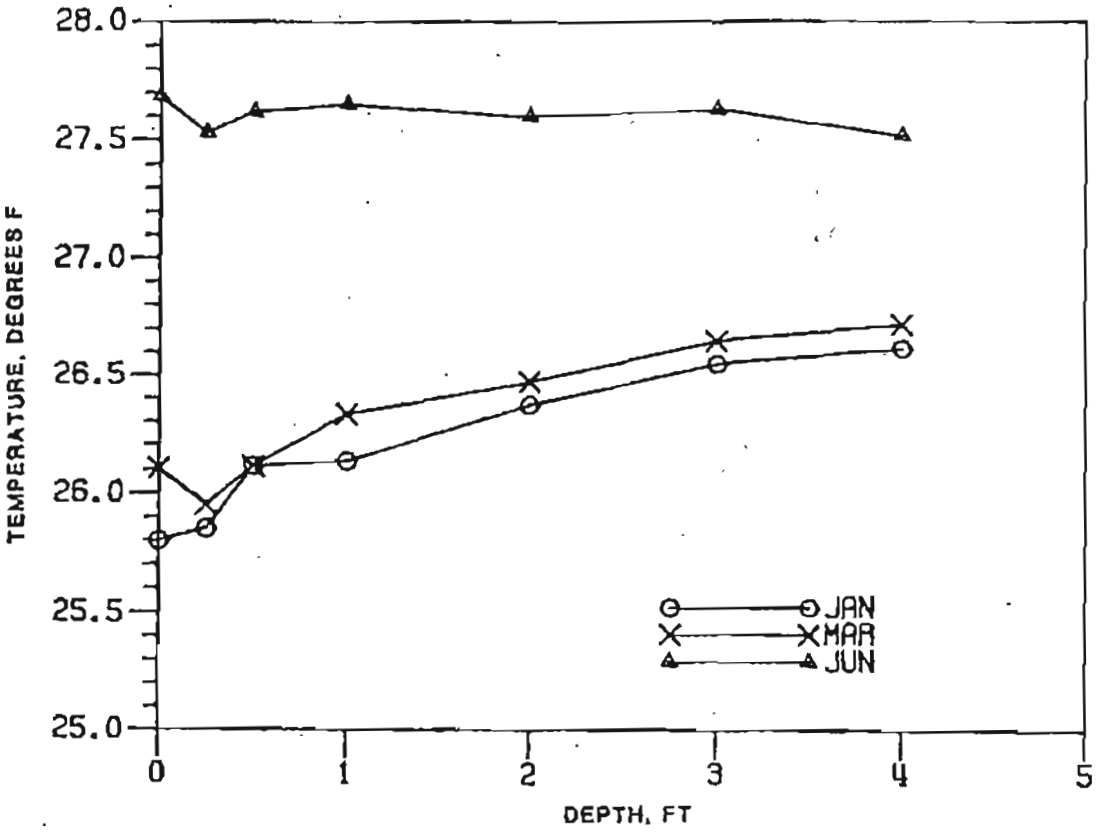

Figure 21. Frozen gravel temperature distribution at one foot depth (January, March and June, 1983).

fects probably only influenced the first one foot of permafrost. After three months of heating, the temperature variation within the gravel decreased, and the thermal transition zone shifted towards a greater depth.

Figures 15 and 16 represent the temperature data of string S6. The trends of curves are similar to those at station S1. The gravel at 4.6 ft. had less temperature disturbance than gravel at 2.6 ft. Figure 14 indicates the temperature variations at station S5. Overall ground temperature of the outside room was 2.5 degrees colder.

Creep Deformation. Creep movements of the USBM gravel room in the tunnel complex resulting from temperature variation were identified for a duration of 180 days. The deformations were taken with a steel tape extensometer (Terrametrics model 50) which had an accuracy of 0.001 in.

Figure 22 and 24 summarizes the observation. The Appendix B tabulates the vertical closure at each convergence station. Stations C1 to C5 were located within the USBM gravel room, and convergence stations C6 to C8 were in the outer compartment.

After installation of these measuring points, readings had been regularly taken at an interval of every 4 days. The convergence information obtained for the period before heating was found to have an average rate of 0.0007 in./day. A large deviation from this creep rate was noted for the readings taken between March 2 to March 6, 1983 (days 47 to 51). The reason for such a large jump is not known. A relatively large temperature oscillation in the month preceding might have created an unstable condition.

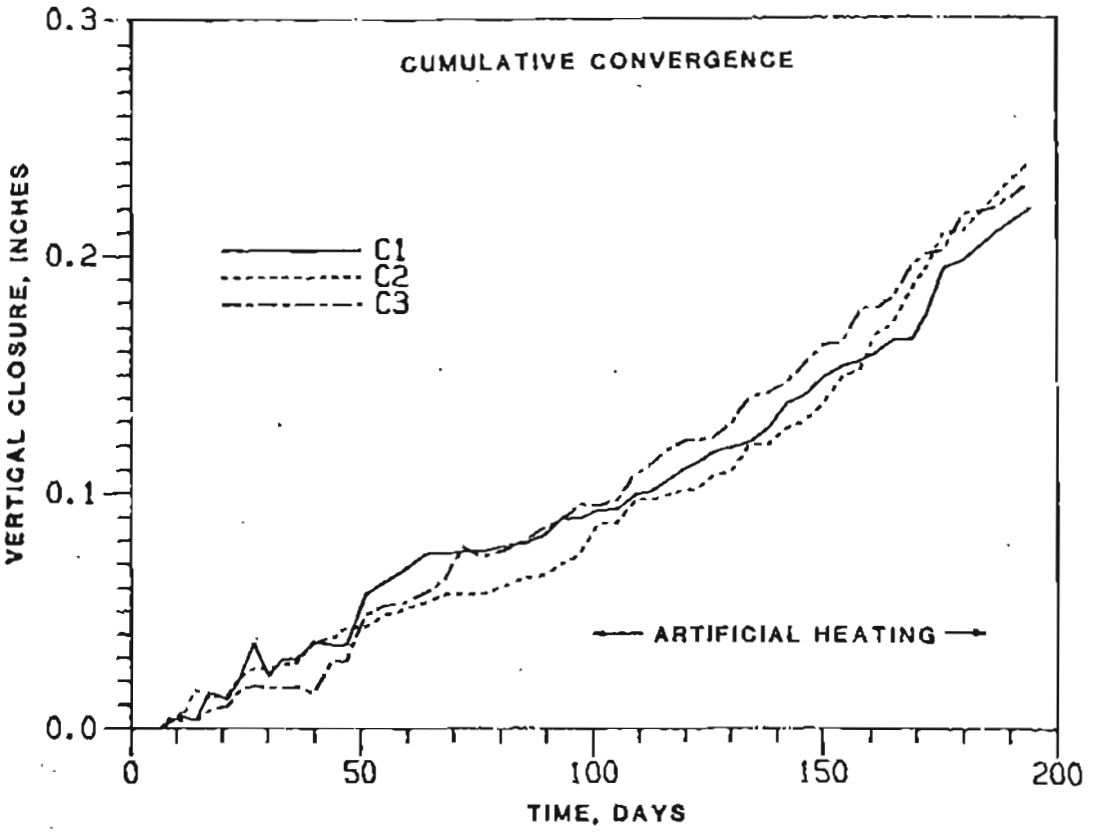

Figure 22. Vertical deformations at convergence stations C1 to C3.

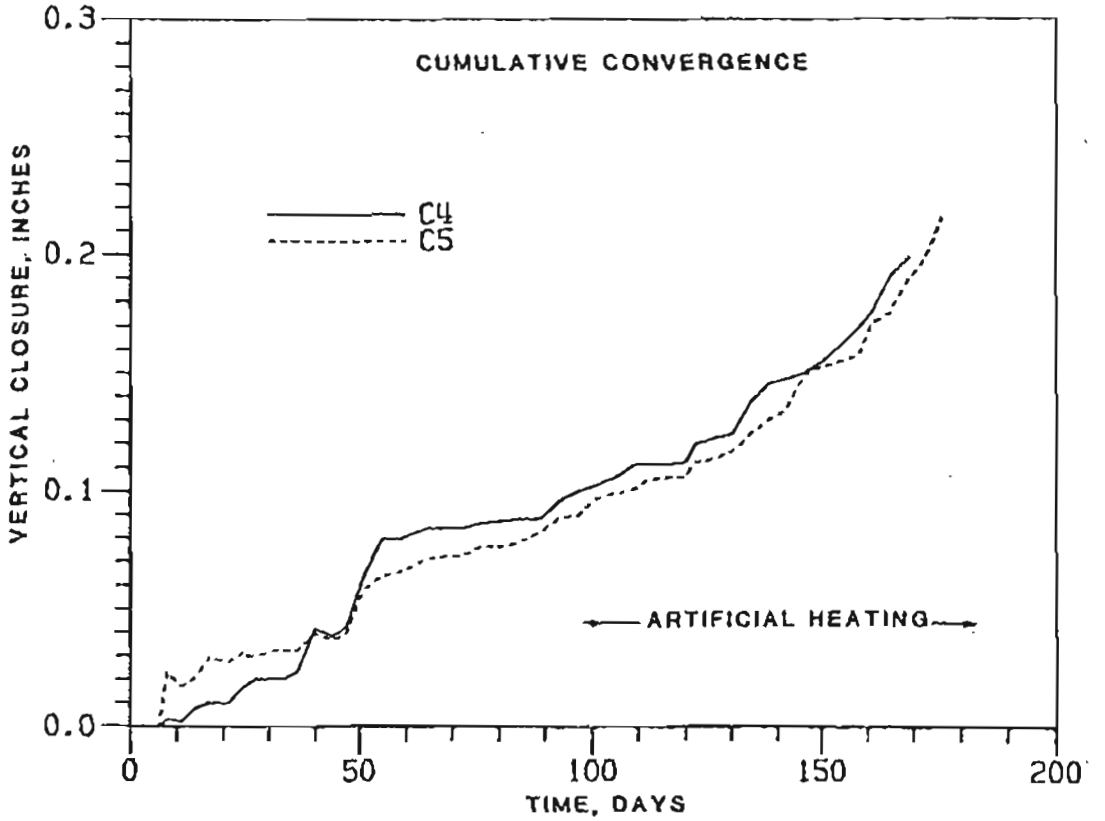

Figure 23. Vertical deformations at convergence stations C4 and C5.

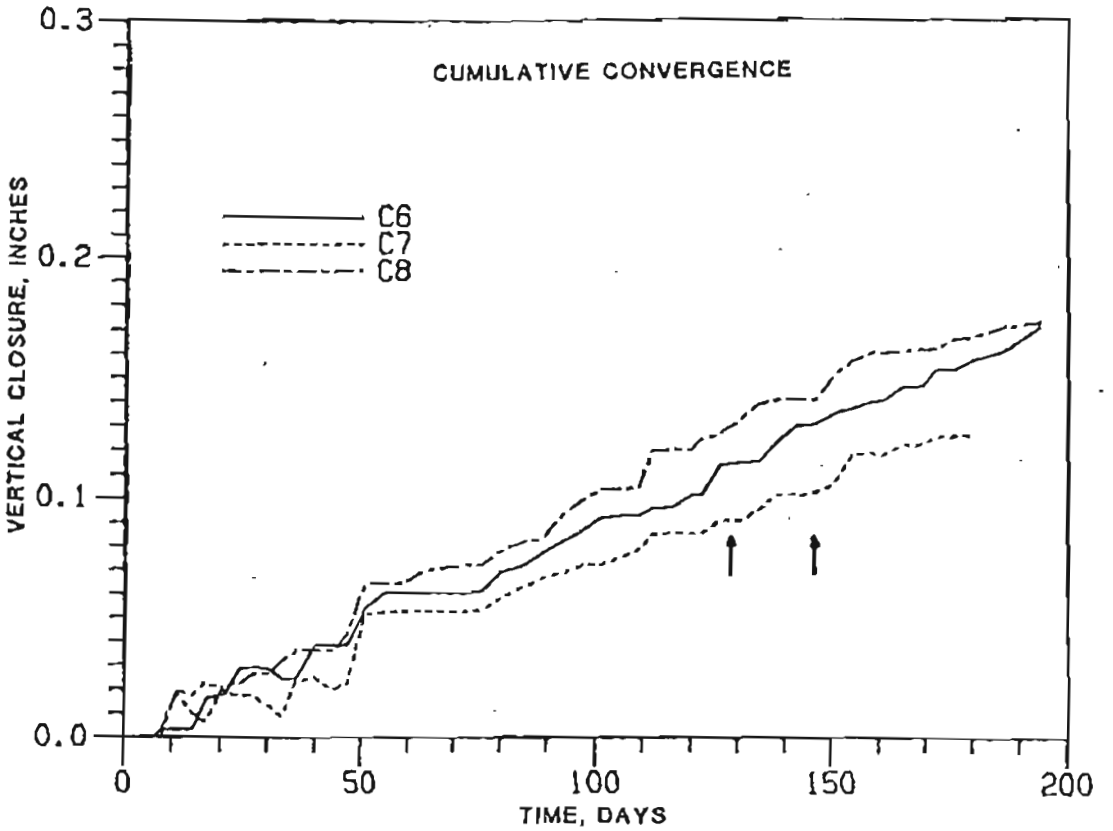

Figure 24. Vertical deformations at convergence stations C6 to C8.

As the steady heating process within the gravel room began, the deformation rate of the roof indicated a significant increase. The heating process started at the refrigeration system was first turned on April 24, 1983. During the first stage of heating, two 150 watt light bulbs were placed on the floor of the room. At the later stage, four lights were used. The energy released from these lights was retained in the room and slowly absorbed by the surrounding ground. For a better illustration of vertical closure changes caused by the heating, the average creep rates for every two weeks at each station were calculated along with average room temperature at 1 foot depth at S3.

The one-foot depth temperature from string 3 was chosen for the analysis. This string was chosen because of its vertical placement in the roof and its proximity to the convergence stations. The depth was selected to represent the thermal history of the roof for that recording period. An analysis of the transient response of a one dimensional, isothermal, semi-infinite, homogeneous medium undergoing a surface temperature step change, was used for the selection. The temperature at a depth, x, and time, t, is given by Johnston (1981) as

$$T(X, t) = T_0 + \Delta T \ \mathrm{erfc}\ X/(4\alpha t)^{\frac{1}{2}} \qquad (1)$$

where T_0 is the initial temperature of the medium, (^oF)

ΔT is the magnitude of the step change, (^oF)

erfc is the complementary error function

α is the thermal diffusivity, (ft^2/hr)

A diffusivity of 0.08 ft^2/hr was estimated from Johnston (1981) for a frozen coarse grained soil with a density of 130 pcf and a 10%

water content. A two degree increase in surface temperature was imposed upon the 26°F medium. This would represent the effect of a two degree increase in room temperature due to either increased activity or a heating element. The results of the analysis are shown in Figure 25. A significant response at less than 1 hour is recognized at a depth shallower than one foot. Short term activities associated with the data recording and tours may have had a significant effect on the shallow thermistor readings. At great depths, the response may be too small or have a significant time lag, causing the reading to have poor correlation with the temperature history of the previous days. The one foot depth, showing a sizeable response after 12 hours was therefore chosen.

A series of regressional analyses was carried out to find the best fitting curve for thermal effects on creep behavior of the frozen ground. The following four models were thought to be reasonably accurate within the testing temperature ranges. They are:

- Linear model

$$C = mT + b \tag{2}$$

- Logarithmic model

$$C = a \ln T + b \tag{3}$$

- Exponential model

$$C = a e^{bT} \tag{4}$$

- Power model

$$C = a T^{b} \tag{5}$$

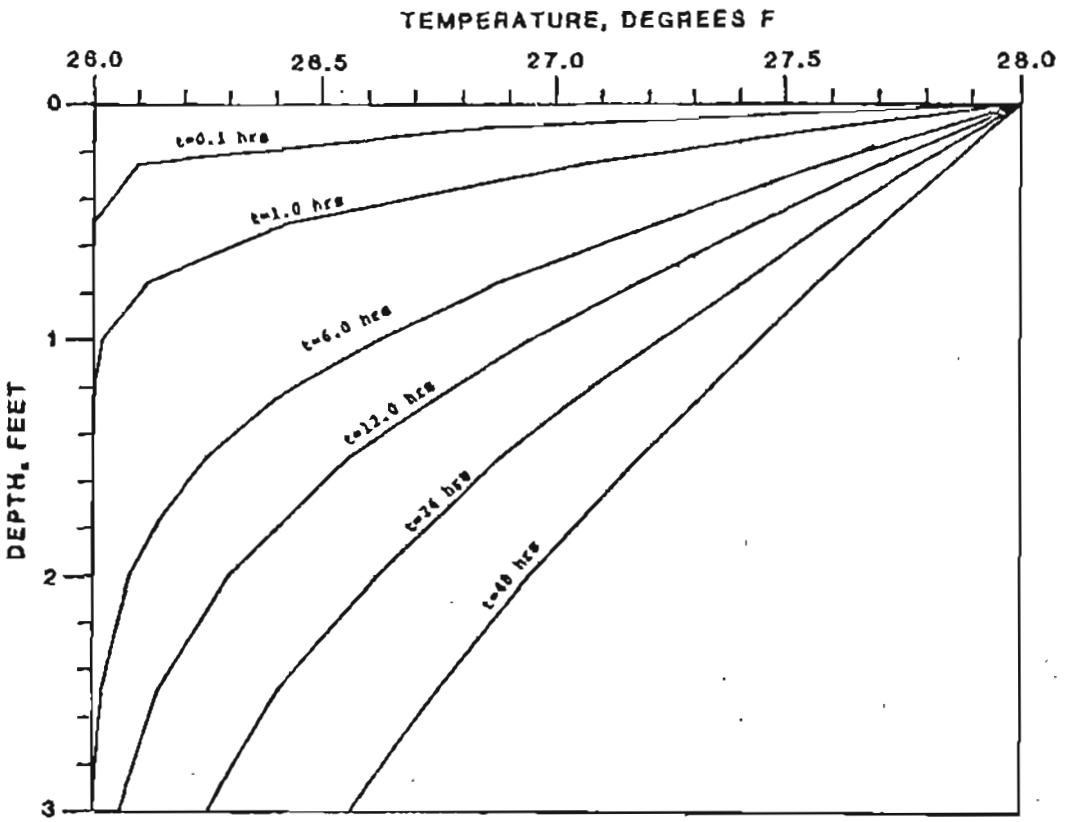

Figure 25. Temperature profiles of frozen gravel obtained from equation (1).

If the boundary conditions are also considered as factors which evaluate the accuracy of the model, the exponential model is superior to the other equations mentioned above. Figures 26 through 30 show the relationships between convergence rate and ground temperature. Table I summarizes the coefficients "a", "b" and the coefficient of correlation (r) of the exponential model for each set of data.

Table I. Summary of regression analysis

Station	a	b	r
C1	3.369×10^{-4}	0.381	0.80
C2	2.206×10^{-5}	0.488	0.81
C3	6.906×10^{-4}	0.360	0.59
C4	6.550×10^{-7}	0.614	0.82
C5	1.086×10^{-6}	0.593	0.83

A randomized block analysis (see Appendix C) was applied to this exponential model in order to identify the influence of geometry and overburden of opening. The calculated F value was 0.70 which indicated the geometric and overburden factor did not significantly influence the observed creep rate in this case. Therefore, the average creep rate of those stations was used to develop an emperical equation which predicts the influence of temperature on behavior of frozen ground in the room (Figure 31). It is:

$$C = 3.2 \times 10^{-5} e^{0.473 T} \quad (6)$$

where C is the convergence rate of gravel roof, (10^{-4} in./day).

e is 2.71828

T is temperature of frozen ground at 1 foot depth, (^{o}F).

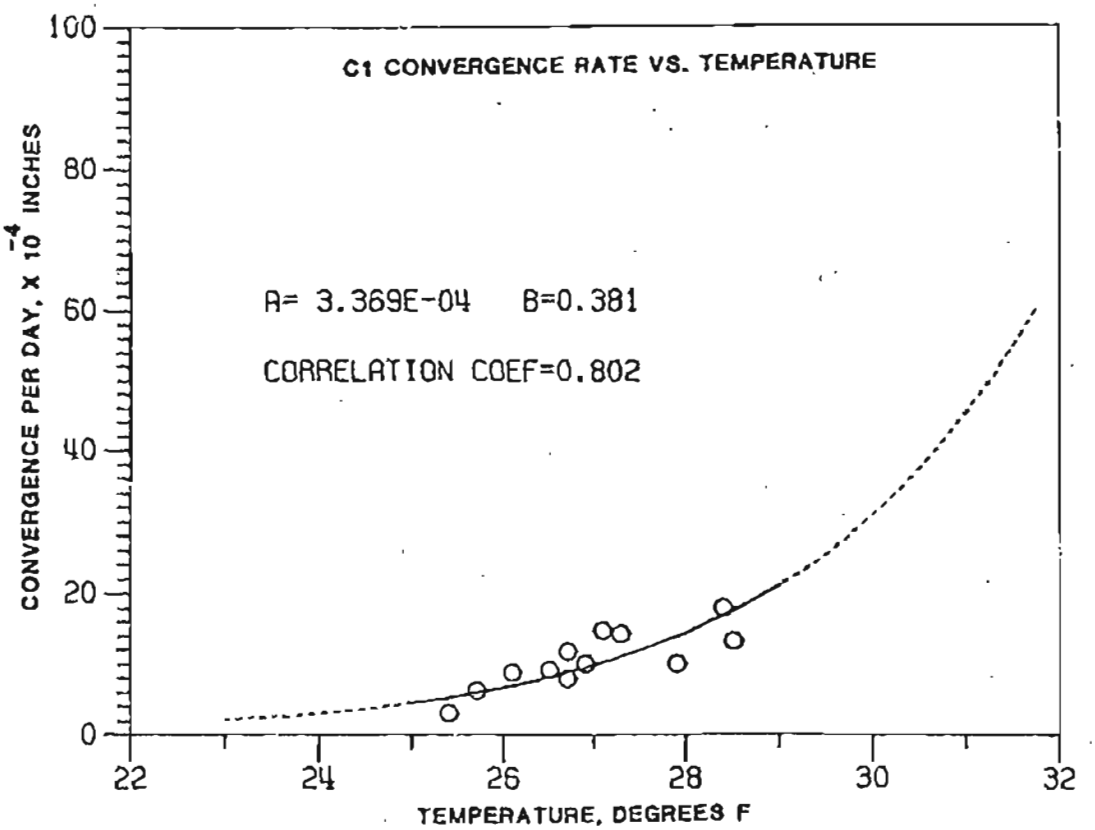

Figure 26. Convergence rate vs. gravel temperature at station C1.

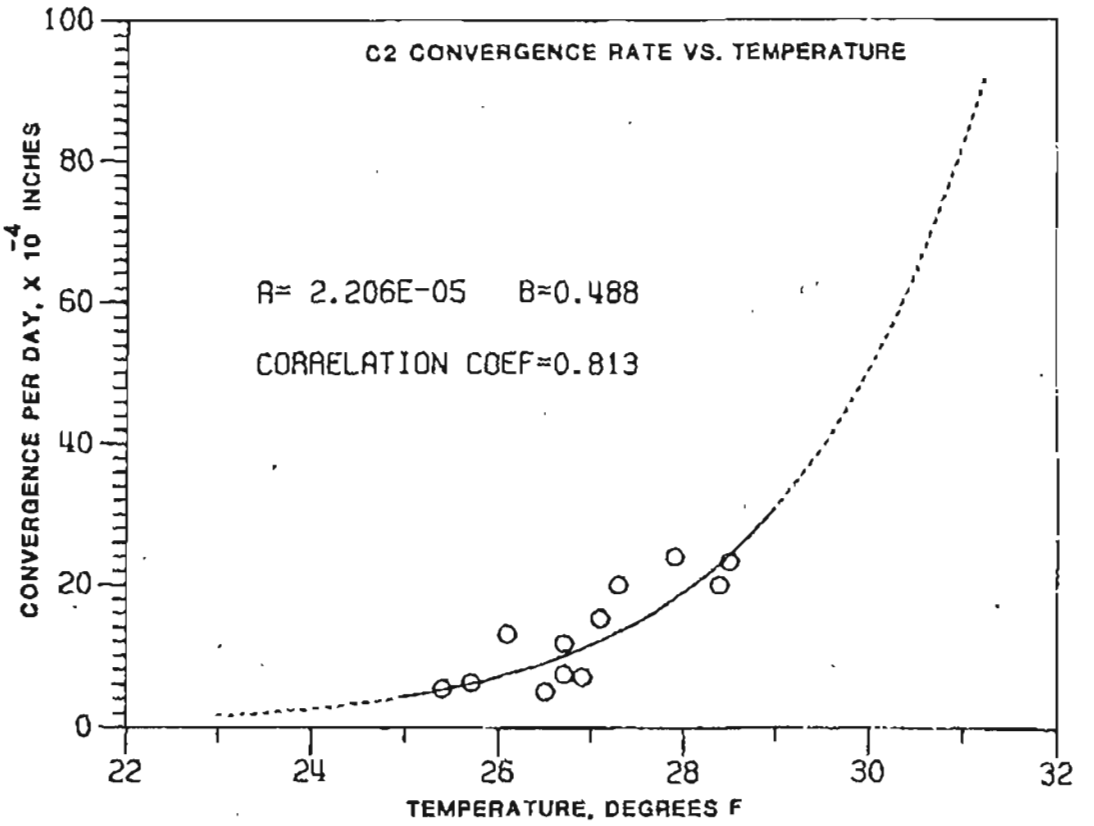

Figure 27. Convergence rate vs. gravel temperature at station C2.

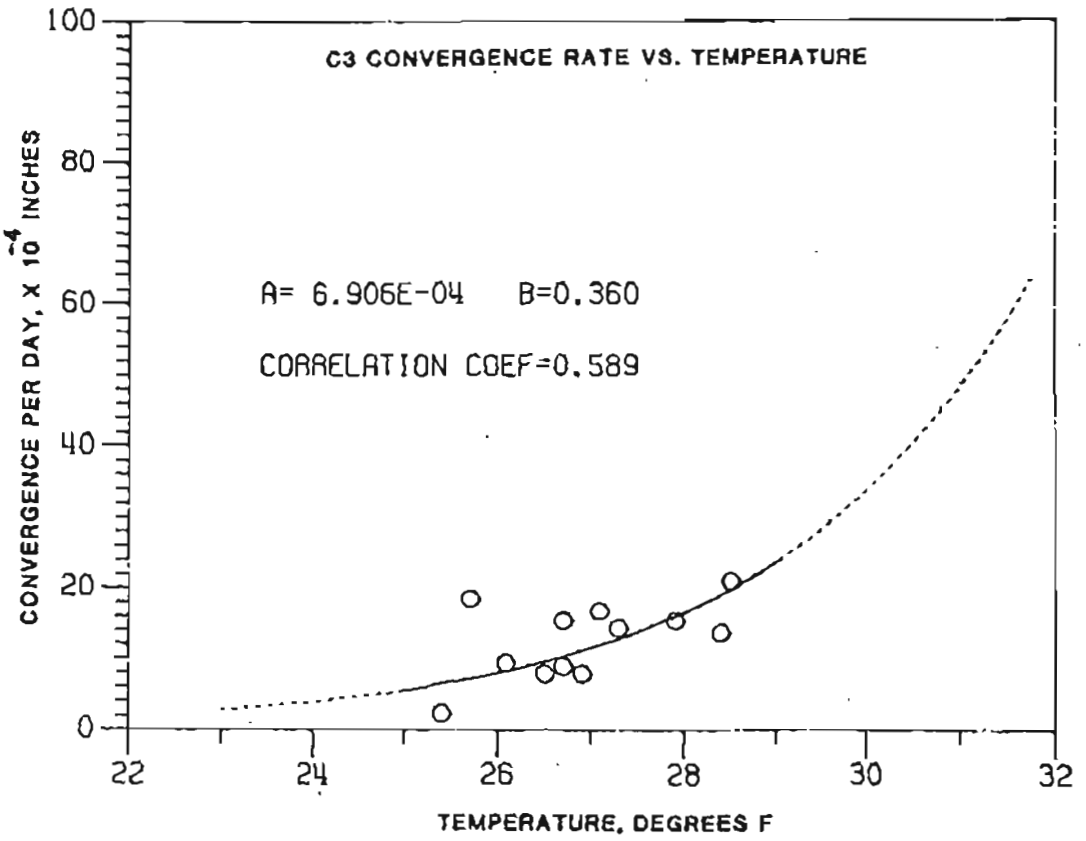

Figure 28. Convergence rate vs. gravel temperature at station C3.

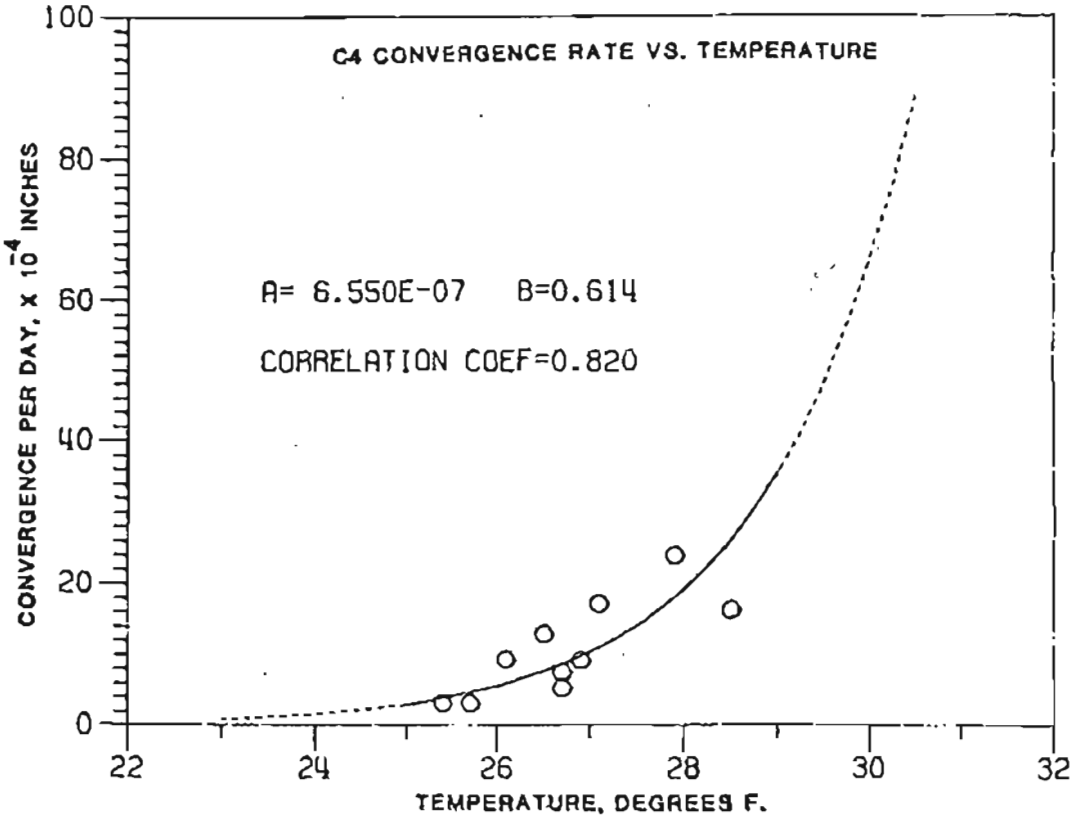

Figure 29. Convergence rate vs. gravel temperature at station C4.

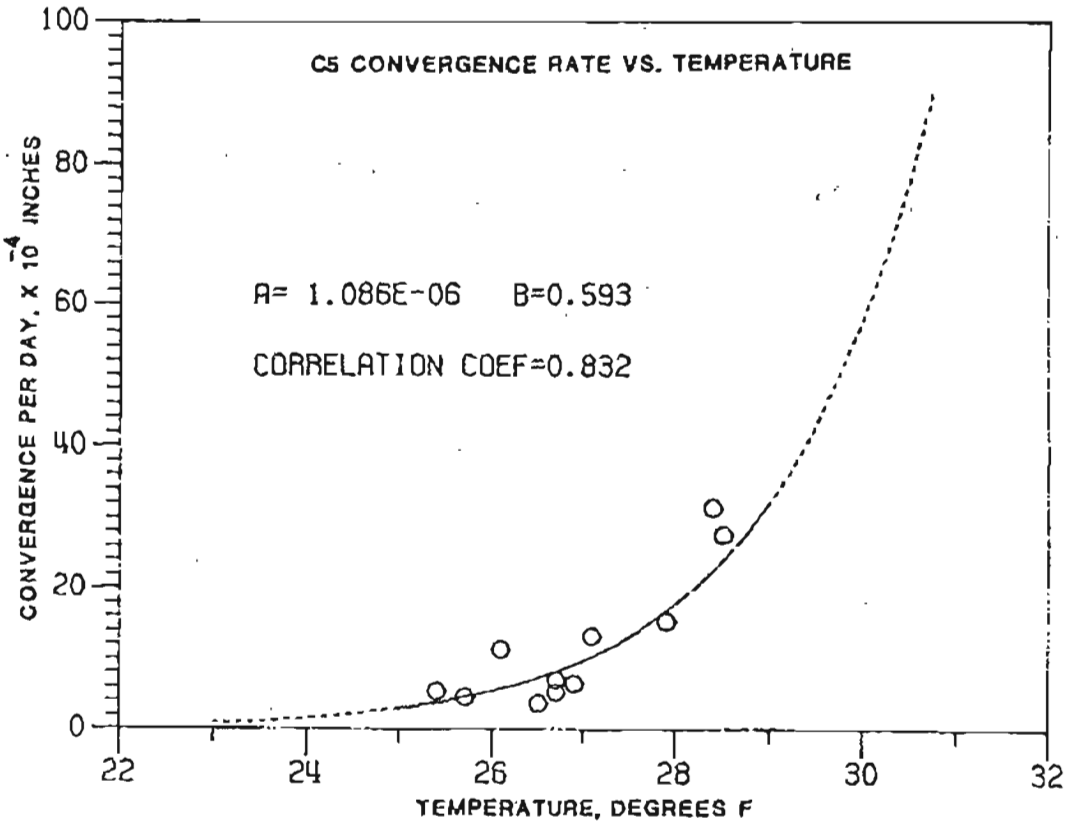

Figure 30. Convergence rate vs. gravel temperature at station C5.

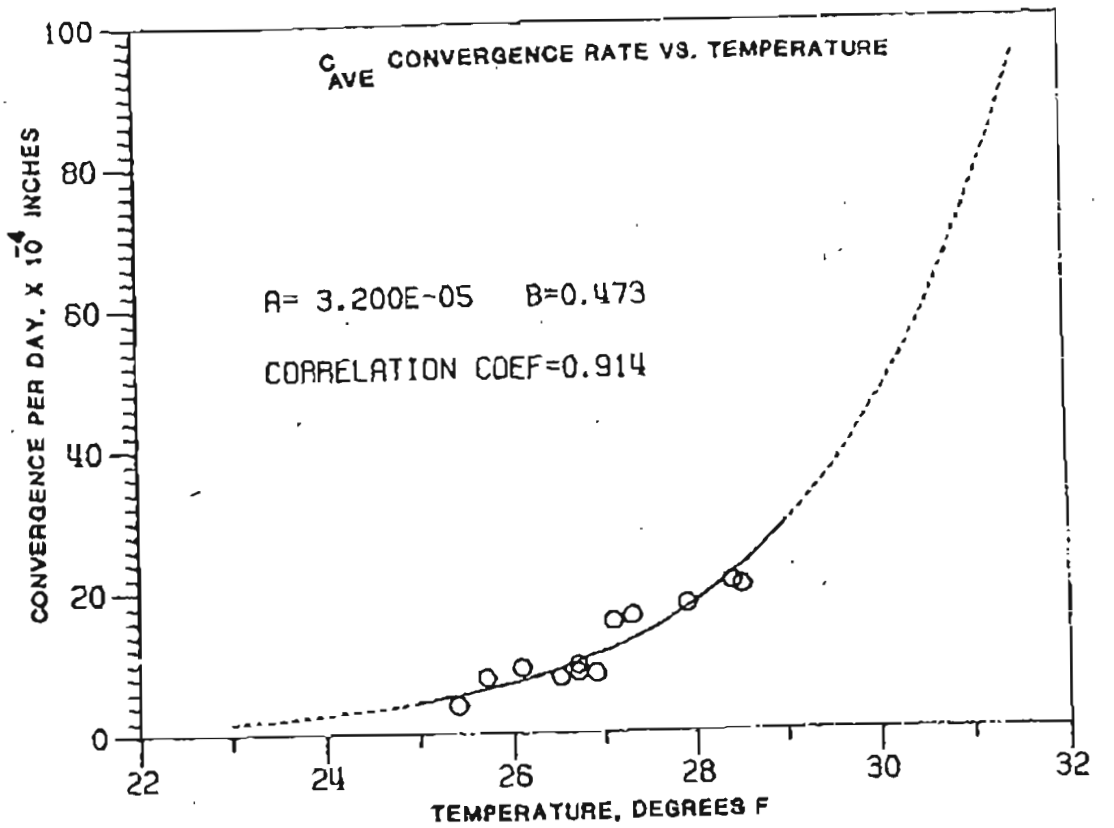

Figure 31. Average convergence rate of the USBM gravel room vs. gravel temperature.

The curve of the equation is subject to modification if more creep information becomes available and a wider temperature range can be achieved. However, a similar trend is believed to exist.

Strata Separation. Strata separations between roof gravel and silt in the gravel room were observed while the air temperature of gravel reached to 29.8°F (Figure 32). An intense heating raised the air temperature to 29.8°F within 4 days duration, then room temperature slowly dropped to 28.6°F in the next 12 days. Later on, the heating process was intensified and air temperature moved up to 29.7°F within one week. After that, the heating source were turned off and the room temperature gradually declined to the background value.

Separation between roof gravel (approx. 6 ft. thick at the M1 station) and silt was observed 5 days after the heating process. During the first rapid heating stage, the average separation rate between anchor #4 (7.5 ft. into the roof) and the head (at the roof surface) was 0.0007 in./day and the rate was reduced to 0.0004 in./day during the second warming-and-cooling cycle. After this the rate decreased to 0.0002 in./day. The anchor #3 (6.5 ft. into the roof) also indicated a small parting (Figure 33). It has been noted from observations that no partings between head and anchors #1 or #2 were recognized. Both anchors 1 and 2 were located in the gravel layer (2.5 ft. and 5.5 ft. into the roof surface). This information indicated the gravel layer most likely acted as a single unit during the heating period.

The M2 extensometer was placed close to the bulkhead inclined at a 20° angle with the vertical. The incline was necessary because of

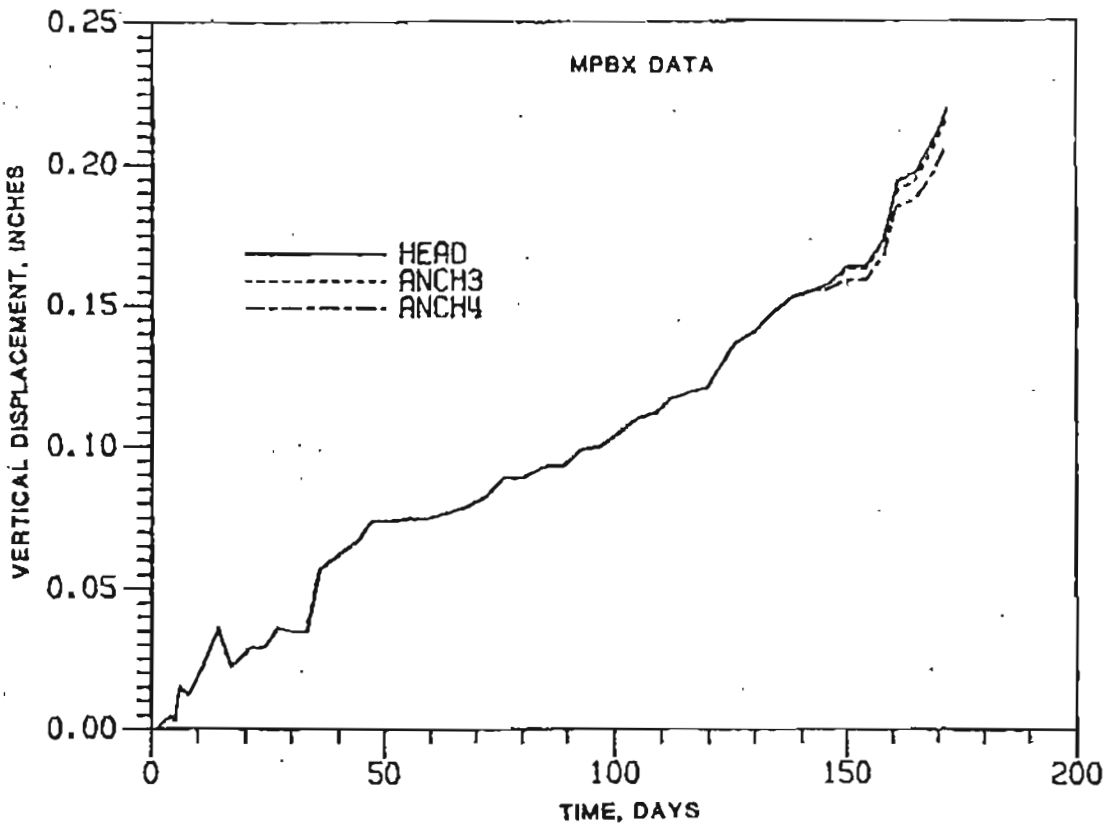

Figure 32. Diagram showing relative movements between anchors and head at MPBX station M1.

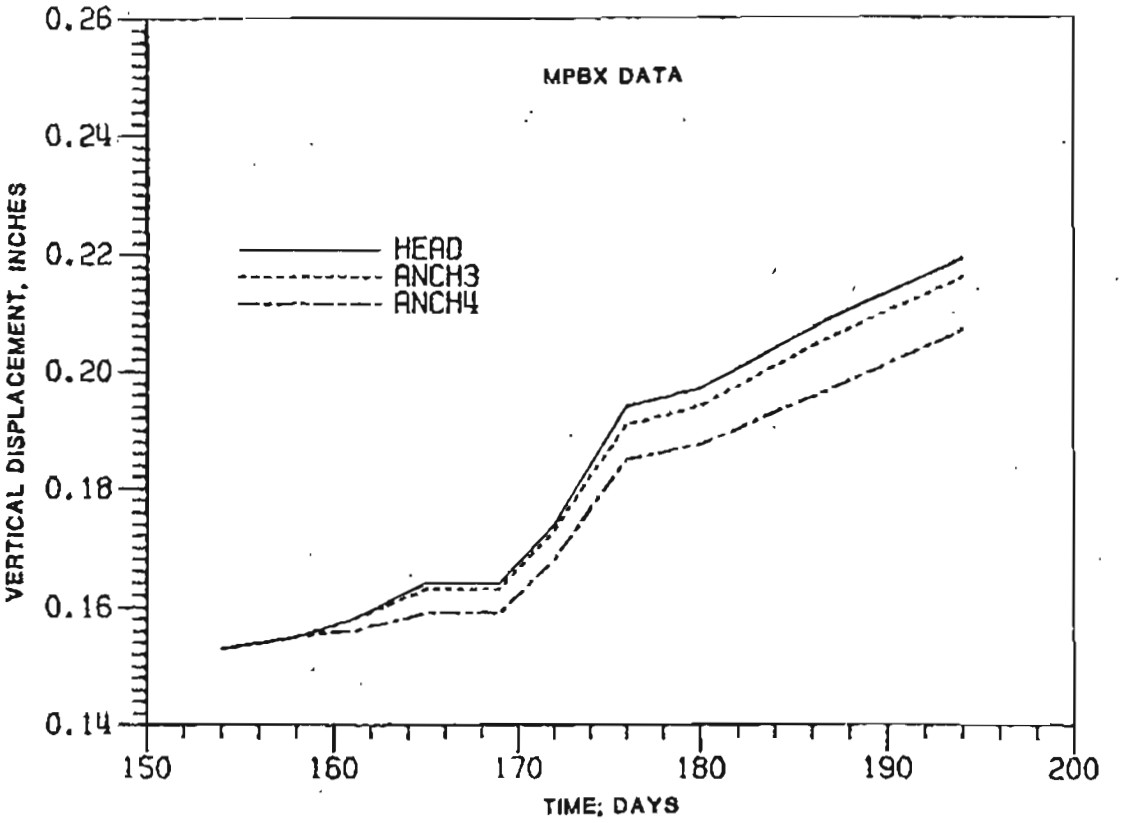

Figure 33. Detailed plot of strata separation at MPBX station M1.

the drilling setup. Data recorded at this station did not indicate any formation separation. The inclined installation might not allow for the sufficient connecting rod freedom necessary for accurate readings.

LABORATORY CREEP TESTS

For engineering applications where the stability of an underground chamber depends upon the strength and deformation characteristics of the in-situ frozen soil, creep behavior must be determined by tests on undisturbed soil samples under stress and temperature conditions which are expected to continue during the life of the structure. Alternatively, field measurements may be required when considerable variability exists in the natural permafrost.

The purpose of these laboratory tests was to investigate the stability of an underground placer mine due to temperature variations. The influence of temperature on creep and long-term strength of frozen ground were evaluated.

Theory

Creep. Vialov and Tsytovich (1955) illustrated the process of creep in frozen soil by considering the condition of applying a constant load to a partially saturated soil mass. This applied load introduces stress concentrations between particle-and-particle contact. As the load continues, surface ice starts to melt under pressure. Differences in water concentration and the stress gradient cause the unfrozen water to diffuse to regions of lower stress and lower water content where it refreezes. The process of ice melting accompanied by water movement breaks the structural bond between ice and soil particle, and results in a time dependent creep phenomenon. This structural deformation readjusts particle arrangements to a denser packing texture, which in turn increases area and number of particle contacts. The process tends to strengthen the frozen soil.

On the other hand, the stress concentration between grain contacts can introduce adverse effects which weaken the structural cohesion and possibly increase the amount of unfrozen water in the frozen soil. The phenomenon is particularly common in fine grained soils. If the applied load does not exceed the long term strength of the frozen soil, then the weakening process is compensated by the strengthening effect. Under such a situation, the deformation rate decreases with time. However, if the applied load exceeds the long term strength of the frozen soil, the breakdown of internal bonds is not completely balanced by the strengthening process and the rate of deformation increases with time. The process eventually develops into visco-plastic stage and causes failure of the soil structures.

The time-dependent deformation characteristics of frozen soil are similar to those creep curves of metals (Figure 34). The primary stage consists of continuously decreasing creep rate. The secondary or steady-state stage is characterized by the minimum but constant creep rate. The final stage is the tertiary stage in which the creep rate accelerates until failure of the soil.

The presence of each stage and its duration depends not only on the constituents of soil, but also on the applied stress levels, and the temperature ranges. At the low stress levels, primary creep dominates. For a stress less than the long term strength of the soil, the creep rate will always reduce to zero, and eventually soil becomes stable. Thus, it is extremely important to determine if the soil stress exceeds the threshold stress level for a particular material.

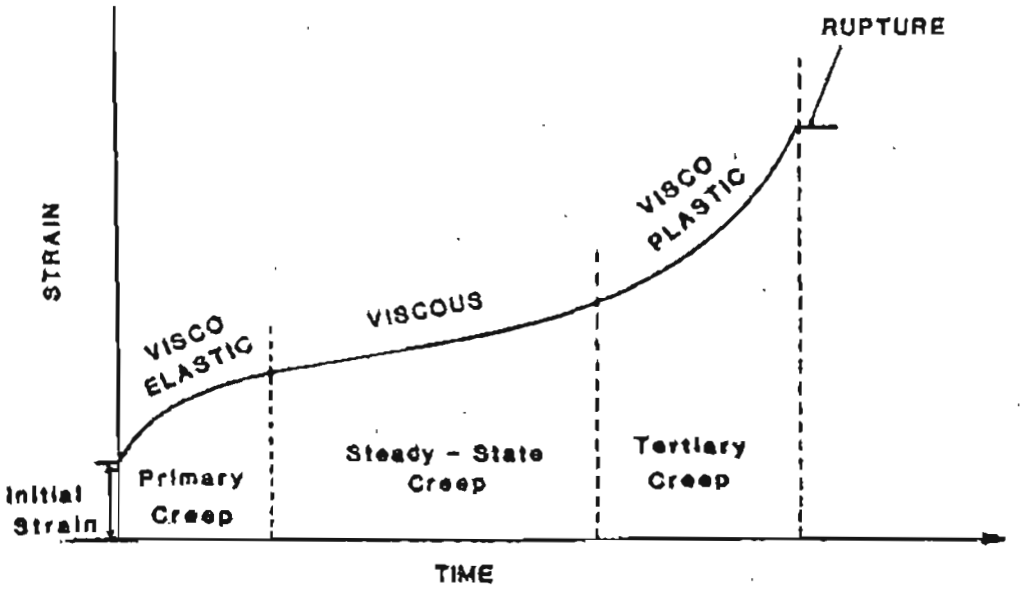

Figure 34. Typical creep curve of frozen soil.

Under moderate stress level the steady-state creep is dominant. When such conditions are present, the weakening process is compensated by the strengthening effect. Many materials undergo large creep deformation during this period without apparent loss of mechanical strength.

For high stress levels, the soil may have a dominant accelerated stage of creep. Under this condition, soil exhibits an almost instantaneous creep deformation.

Strength. Strength of frozen soil, similar to the unfrozen cohesion soils, depends upon the cohesion and the internal friction of the mass. According to Vialov and Tsytovich (1955) the cohesion of frozen soil consists of: (1) the attractive forces between particles; (2) physical or chemical cementing of particles; and (3) bonding of soil particles by ice crystals in the voids. Cementation of grains by ice is the dominant strength factor in frozen soil even though the soil particles are surrounded by a film of unfrozen water. The ice cohesion is dependent upon the amount of ice, the strength of ice crystal, the area of ice in contact with the particle and soil temperature.

Cold Laboratory Facility

Unsaturated soil specimens were frozen and tested in a walk-in type cold room in the University of Alaska, Fairbanks. The temperature of cold laboratory was controlled to within $\pm$ 2.0^{o}F by means of a thermostat. The defrost system was turned on for a couple of minutes every hour of testing in order to remove accumulated moisture. During the defrost cycle room temperature was up by one or two degrees.

Specimen Preparation

The testing soils were sampled directly from the USBM gravel room of the USA CRREL tunnel. Particles passing through a 0.5 inche sieve were collected and saturated in a cold water bath overnight. Figure 35 shows the particle distributions of natural soil and the remolded specimens. The curves 911A and 911B indicate the particle ranges of natural frozen gravel. Both samples show that the majority of grains is in large sand size. Curves CR25 and CR29 indicate the particle sizes of specimen CR25 and CR29 which were tested at 25°F and 29°F respectively. Those particle distributions were very similar to those of the natural gravel except in the larger particle size. The existence of particles larger than 0.5 inches in diameter caused minor testing problems. The large grains generated premature failure of samples under loading, therefore, it was necessary to sort out the large particles.

Later, the soil particles were placed in an aluminum (6 in. diameter and 12 in. height) mold in three equal layers. The first layer of soil was tamped 20 times with a standarized Proctor tamping rod. The other two layers were compacted 25 times each. After the mold was filled with soil the specimen was placed in a sink and was saturated from the top by allowing a small amount of water dripping through the sample for several hours. When the saturation process was completed, the sample was brought to the cold room. The top surface of specimen was wrapped with a battery blanket (80 watts) and the top half of the soil sample was insulated with fiberglass. On top of the battery blanket a layer of styrofoam was applied to ensure a uniform

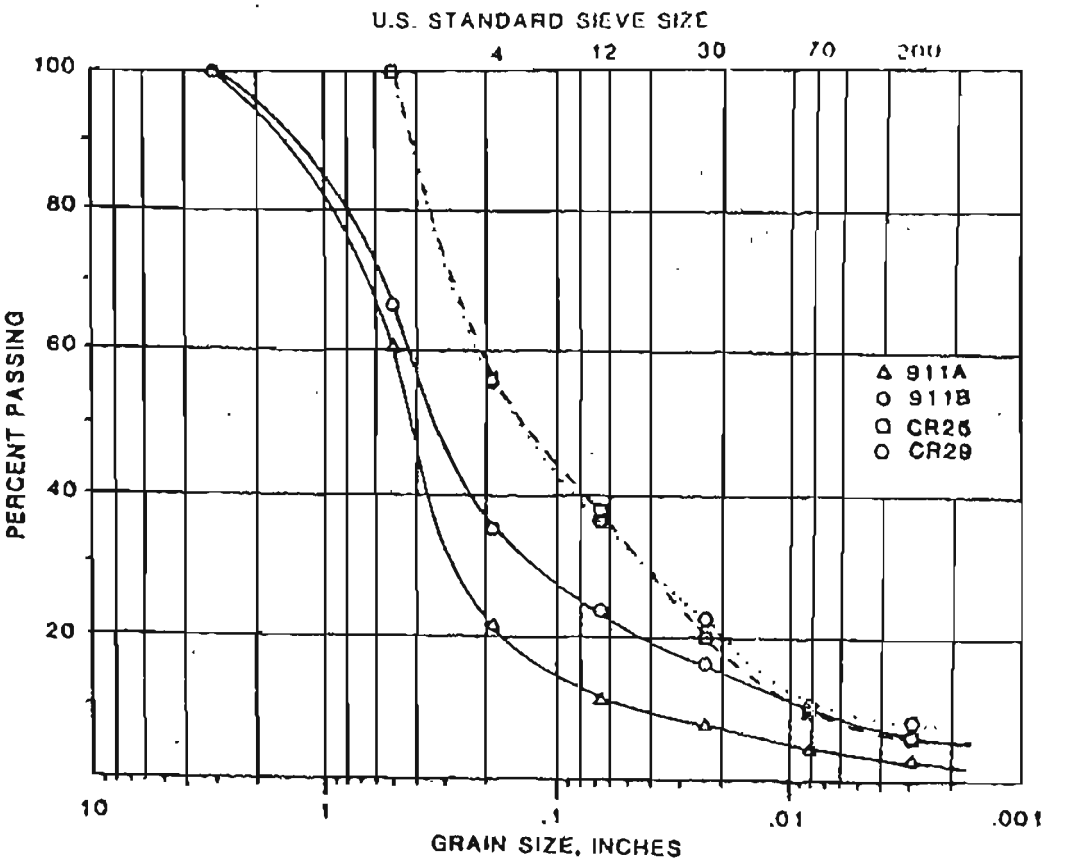

Figure 35. Particle size distribution curves of natural frozen gravel and testing specimens.

thermal regime at the top end of the sample. The battery blanket was turned on for 3 hours when the cold room temperature was 25°F and it was on for 6 hours when the cold laboratory was 29°F. With this arrangement the freezing front moved from the bottom to the top of the specimen. This one directional process allowed the entrapped air to escape and prevented the unnecessary heave of sample. Soil samples were frozen within a period of one or two days.

Before removing the frozen specimens from the mold, a fine layer of silt slurry was sprayed on the top end of the sample to obtain a smooth surface. The thin layer of silt avoided local stress concentrations at the relatively large sand and gravel grains in contact with the loading platen. After the slurry froze, the specimen was removed from the freezing mold for creep testing.

Testing Procedures and Results

Creep test was performed at constant stress level of approximately 18% of the uniaxial compressive strength under specific temperature. The 18% of the unconfined compressive strength was selected because the long term strength of frozen soil is usually less than 20% of the unconfined compressive strength (Andersland and Anderson, 1978). Both tests were performed on specimens with 6.0 inches diameter and 12.0 inches height. A summary of individual specimen data is shown in Table II.

The loading device used in the testing program is shown in Figure 36. The loads was applied to the test specimen by means of a 10,000 lb. mechanical screw jack. The magnitude of the force was recorded with a 50,000 lb. load cell. During the test, applied load was

Table II. Material properties of testing specimens

	Testing Temp. (°F)	Particle size finer than 0.5"	#4	#10	#30	#70	#100	W (%)	Ave. stress level (psi)	Ave. Unconf. strength (psi)
CR 25	25	100	56.4	38.6	21.1	10.0	6.3	10.1	212	1178
CR 29	29	100	55.9	36.2	23.1	11.6	7.4	11.8	153	846

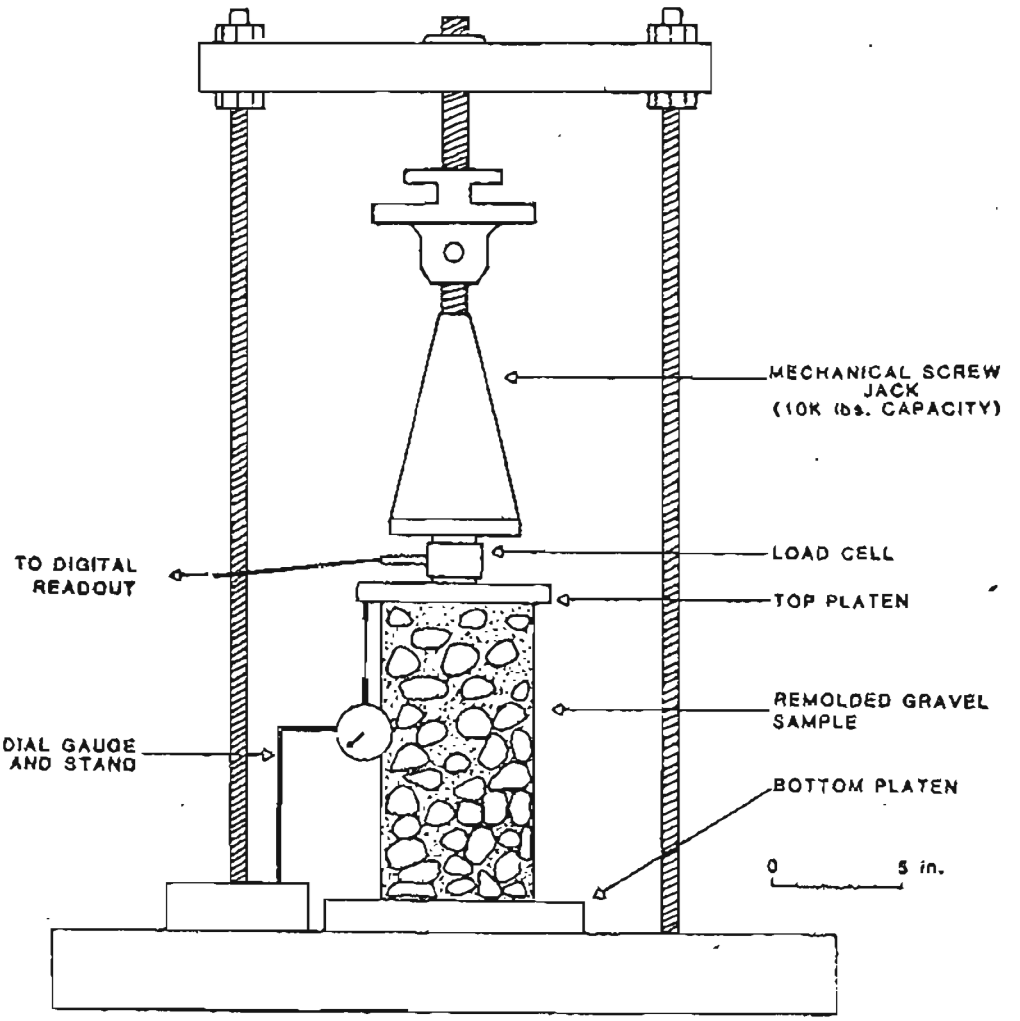

Figure 36. Creep test apparatus.

manually adjusted to the predesigned magnitude. Average axial deformations of test specimens in the creep test were measured using two dial gauges (0.001 inches sensitivity) mounted on the loading frame. Deformation and applied load were checked frequently for a period of one week.

Data from the laboratory test are shown in Figure 37. The time-strain curve CR25 summarizes the data for unsaturated frozen gravel subjected to creep test at 25°F under 212 psi of average applied stress. The initial strain was 7×10^{-3} which occurred almost instantaneously. Data for the curve showed a typical example where primary creep is dominant. The curve asymptotically approaches a constant deformation. The curve CR29 indicates time-strain data for the gravel specimen loaded with 153 psi of stress at 29°F. The initial strain was about 7×10^{-3} which was similar to that observed in CR25. The specimen displayed only primary creep during one week of testing. The axial strain of CR29 was about 1.6 times greater than the strain of CR25. The large difference occurred within the first three days.

For easier illustration of creep behavior of frozen specimens, the strain rates were plotted. Strain rates were determined as the slopes of the strain vs. time curves. The rates for each testing specimen were computed by averaging three consecutive data points on the time-strain curve.

New groups of three data points were considered by advancing along the time-strain curve one point at a time. This process was repeated for the entire set of data. Typical strain rate vs. time curves for specimens CR25 and CR29 are plotted on Figure 38. Both

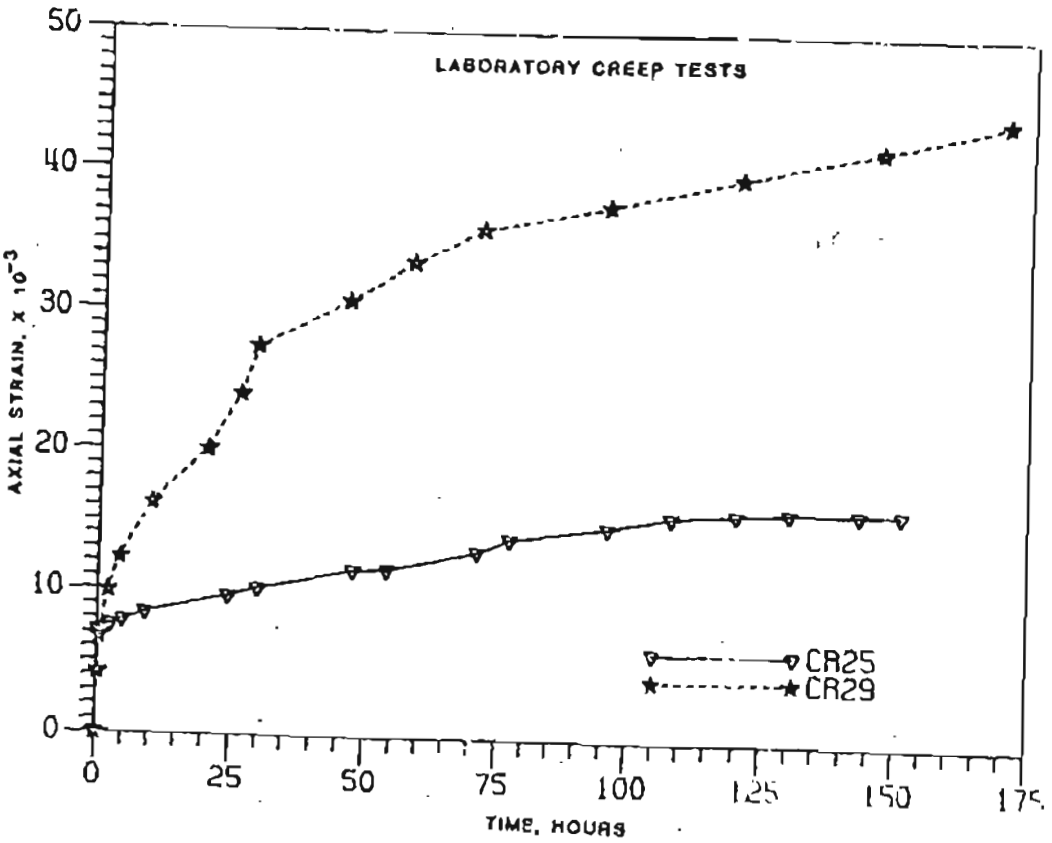

Figure 37. Results of laboratory creep tests for frozen gravel at 25° and 29°F.

damped creep curves have high initial strain rates which decrease hyperbolically during primary creep stage and approach the zero rate.

As noted from Figure 38, the creep rate of CR29 was two to three times the amount recorded for CR25 which averaged around 0.00025/hr. during the first three days. After then, both samples had very similar creep rates.

The primary creep of frozen soil under constant stress at constant temperature is dependent upon temperature and material type. The creep strain can be described by the creep law.

$$\varepsilon^{(c)} = Ct^{b} \tag{7}$$

And, the creep rate can be presented as follows:

$$\dot{\varepsilon}^{(c)} = C't^{b'} \tag{8}$$

where

C is a constant $\{= (\frac{\dot{\varepsilon}_c}{b})^{b} (\frac{\sigma}{\sigma_c})^{n}\}$

t is the time

$\dot{\varepsilon}_c$ is an arbitrarily selected creep rate ($=10^{-5}$ min^{-1})

σ is the uniaxial normal stress applied.

σ_c is the material creep modulus $\{= \frac{(\dot{\varepsilon}_c/b)^{b}}{c_0}^{1/n}\}$

n, b are temperature dependent material constants.

C', b' are temperature dependent material constants (C' = Cb and b' = b - 1)

Evaluation of b and C for a given frozen soil can be made if the experimental creep strain and time data linearize on a plot of log ε vs. log t. Also the parameters b' and C' can be determined by plotting the log $\dot{\varepsilon}$ vs. log t. The parameters n and σ_c are evaluated

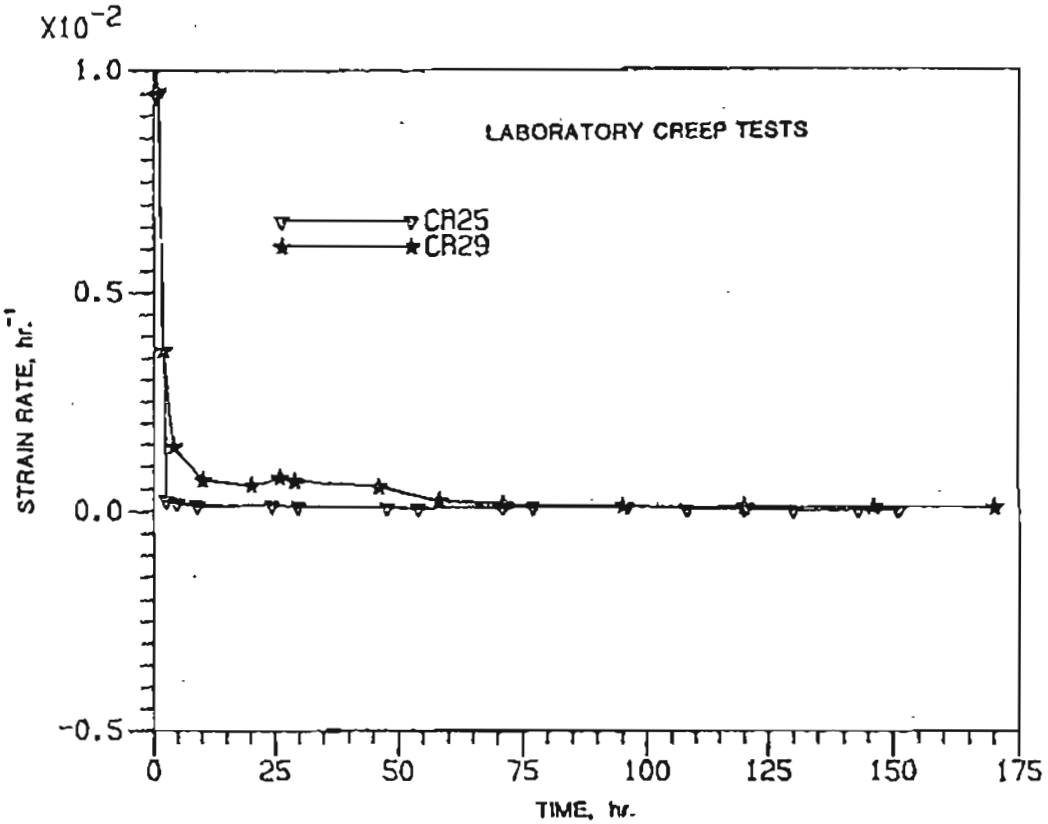

Figure 38. Creep strain rate and time for frozen gravel at 25° and 29°F.

by plotting the different values of applied stress (σ) vs. the corresponding values of C derived from log t - log ε or log t - log $\dot{\varepsilon}$ diagram on a log-log coordinates. The slope of log σ - log C indicates the value of parameter n. With the estimated parameters the creep modulus of frozen soil at a given temperature can therefore be determined.

Figure 39 shows the strain vs. time curves for CR25 and CR29 plotted on log-log coordinates. By intercepting the linear line with Y-axis at time = 1 hr., the constant C was calculated. The C value for frozen gravel for sample CR25 was 0.005656 and was 0.007859 for CR29. Slopes of the lines represent the material constant b. The coefficient b was 0.200558 for CR25 and was 0.343845 for CR29.

The strain rate vs. time curves for the samples was also plotted on log-log scales (Figure 40). The constants C' and b' were estimated directly from the curves. The b' values calculated from the slope of the time-strain rate curves were - 0.344506 and - 0.830102 for specimen CR25 and CR29 respectively. The coefficient C' was 0.000284 for CR25 and was 0.006372 for CR29. The summarized statistical data are listed in Table III. It is interesting to note from the diagram that the gradient of strain rate was also a temperature dependent factor. The CR29 curve indicates a greater change of strain rate than that of CR25. Both curves intercept at 631 hours when the rate approaches 31.32 x 10^{-6}/hr.

The imposed primary creep and creep rate of frozen gravel by 212 psi of stress at 25°F can therefore be described as follows:

$$\varepsilon^{(c)} = 0.005656 \quad t^{0.200558} \tag{9}$$

and $$\dot{\varepsilon}^{(c)} = 0.000284 \quad t^{-0.344506} \tag{10}$$

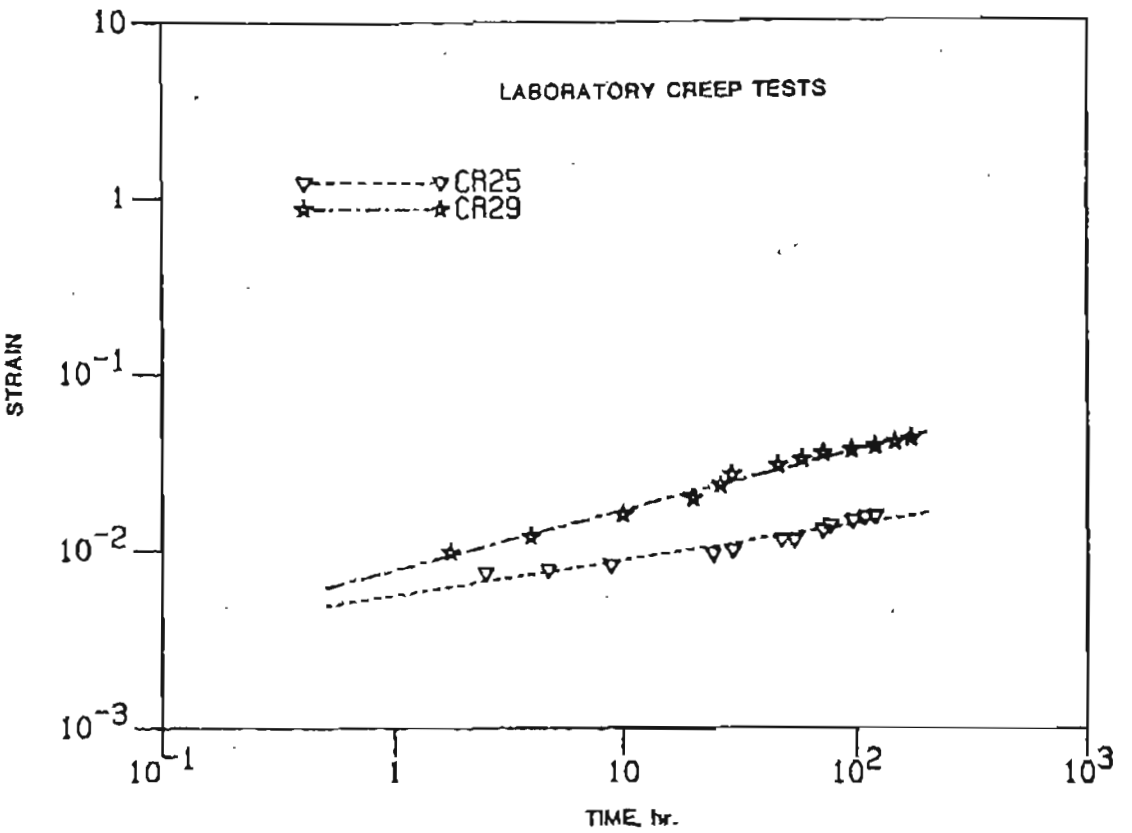

Figure 39. Primary creep strain vs. time for frozen gravel at 25° and 29°F.

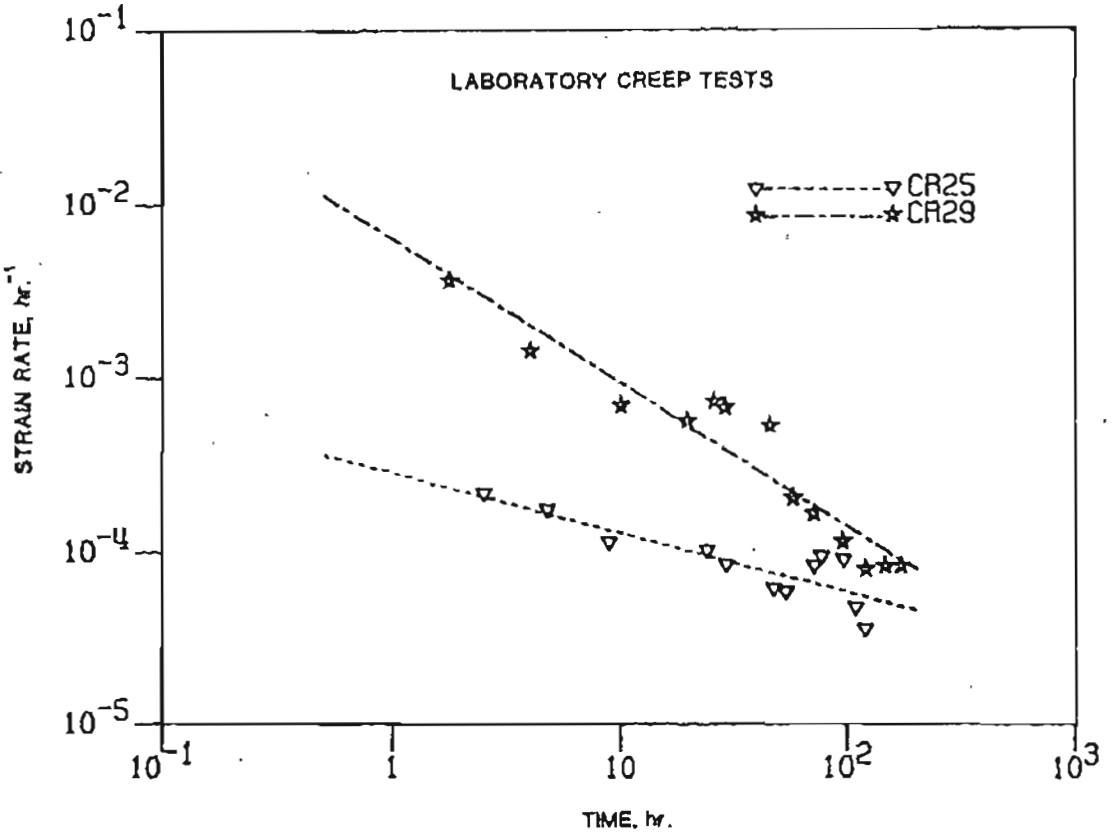

Figure 40. Primary creep strain rate vs. time for frozen gravel at 25° and 29°F.

Table III. Temperature dependent material constants

Sample	Strain C x 10^{-3}	Constant b x 10^{-3}	Correlation coefficient	Strain Rate C' x 10^{-3}	Constant b' x 10^{-3}	Correlation coefficient
CR25	5.656	200.558	0.96	0.284	-344.506	-0.95
CR29	7.859	343.845	0.99	6.372	-830.102	-0.86

The primary creep and creep rate due to a 153 psi of applied stress at 29°F are:

$$\varepsilon^{(c)} = 0.007859 \quad t\ 0.343845 \tag{11}$$

and $$\dot{\varepsilon}^{(c)} = 0.006372 \quad t^{-0.830102} \tag{12}$$

where $\varepsilon^{(c)}$ is the creep strain at a given temperature and stress.

$\dot{\varepsilon}^{(c)}$ is the creep strain rate

t is the time, (hr).

CONCLUSIONS

An unsupported underground chamber constructed in a perennially frozen soil is feasible if the thermal properties of materials are understood and thermal disturbance in the area is minimal. The experience gained from this study has shown that the cyclic heating and cooling effect introduced more instability of ground than the other factors. Changes of ground temperatures can exponentially increase or decrease the long term deformation of opening.

Data from field monitoring indicated that the average long term creep rate of frozen gravel in the tunnel site was about 0.001 in./day. The creep rate of gravel room changes with variations of ground temperature and it can be predicted by the following empirical equation:

$$C = 3.2 \times 10^{-5} e^{0.473T}$$

where C is the convergence rate in 10^{-4} in./day and T is the temperature of frozen ground at one foot depth in ^{o}F.

Separation of the roof gravel and silt was observed as three months of heating increased the gravel temperature by one degree. The average separation rate was 0.0007 in./day during the heating stage. It decreased to 0.0002 in./day as the heating process was slowed down gradually. Separation within the roof gravel was not noticed. It is very likely that the 6 ft. gravel behaves as a single unit.

The factors affecting the creep characteristics obtained from laboratory tests on remolded frozen gravel are temperature and the applied stress. The tests indicated that frozen gravel under 18% of

unconfined compressive strength exhibited a primary creep dominant stage. The results of this laboratory test show that

a. the primary creep of frozen gravel loaded under 18% of the unconfined compressive strength at 25°F can be predicted by the empirical equation.

$$\varepsilon^{(c)} = 0.005656\ t^{0.200558}$$

and for frozen gravel at 29°F:

$$\varepsilon^{(c)} = 0.007859\ t^{0.343845}$$

where $\varepsilon^{(c)}$ is creep strain and t is in hours.

b. the primary creep rate is temperature and stress dependent. It can be estimated by the following equation at 25°F:

$$\dot{\varepsilon}^{(c)} = 0.000284\ t^{-0.344506}$$

and at 29°F:

$$\dot{\varepsilon}^{(c)} = 0.006372\ t^{-0.830102}$$

where $\dot{\varepsilon}^{(c)}$ is the creep strain rate and t is in hours.

The findings obtained from the laboratory tests also indicate that the axial strain of specimen CR29 was about 1.6 times greater than that of CR25, even the applied pressure to the CR29 was only 72% of that loaded to the CR25.

REFERENCES

Andersland, O.B. and Anderson, D.M., Geotechnical Engineering for Cold Regions, McGraw-Hill Book, New York, N.Y.. 1978.

Davis, O.L., The Design and Analysis of Industrial Experiments, 2nd edition, Longman Group Ltd., London, Great Britian, 1979.

Johnston, G.H., Permafrost: Engineering Design and Construction, John Wiley & Sons, New York, N.Y., 1981.

Pettibone, H.C. and Waddell, G.G., "Stability of an Underground Room in Frozen Gold-Bearing Strata, Fairbanks, Alaska," 75th Annual Northwest Mining Association Convention, Spokane, WA, Dec. 1969.

Sayles, F.H., "Creep of Frozen Sand", USA CRREL Technical Report TR 190, 1968.

Sellers, J.B., "The measurement of rock stress changes using hydraulic borehole gages", Int. J. Rock Mech. Min. Sci., vol. 7, pp. 423-435, 1970.

Sellmann, P.V.. "Geology of the USA CRREL Permafrost Tunnel, Fairbanks, Alaska," USA CRREL Technical Report TR 199, 1967.

_____, "Geology and Properties of Materials Exposed in the USA CRREL Permafrost Tunnel," USA CRREL Special Report SR 177, 1972.

Thompson, E.G. and Sayles, F.H., "In-situ Creep Analysis of Room in Frozen Soil," Journal of the Soil Mechanics and Foundation Division, ASCE, Vol. 98, No. SM9, Proc. paper 9202, Sept. 1972, pp. 899-915.

Tsytovich, N.A., The mechanics of frozen ground, McGraw-Hill Book, New York, N.Y., 1975.

APPENDIX A

Summary of Temperature Data

STRING# 1 NO. OF THERMISTORS 7

THERMISTOR POSITION	TH140 4.0'	TH130 3.0'	TH120 2.0'	TH110 1.0'	TH105 0.5'	TH103 .25'	TH100 0.0'
DATE	TEMPERATURE						
1.15	26.6	26.4	26.1	25.8	25.5	25.3	25.4
1.16	26.5	26.4	26.1	25.9	25.7	25.5	25.6
1.18	26.6	26.5	26.3	26.1	25.9	25.7	25.8
1.19	26.6	26.5	26.3	26.1	26.0	25.8	25.9
1.20	26.6	26.5	26.3	26.2	26.0	25.8	25.9
1.22	26.6	26.6	26.4	26.2	26.0	25.9	26.0
1.25	26.6	26.6	26.5	26.4	26.2	26.1	26.2
1.28	26.7	26.7	26.6	26.9	26.5	26.3	26.5
1.31	26.8	26.8	26.7	26.7	26.6	26.5	26.6
2.04	26.9	26.9	26.8	26.7	26.6	26.5	26.8
2.07	26.9	27.0	26.9	26.9	26.8	26.7	26.8
2.10	27.0	27.0	26.9	26.8	26.9	26.7	26.6
2.13	26.9	26.9	26.8	26.6	26.3	26.1	26.1
2.16	26.8	26.8	26.2	25.7	25.3	25.1	25.1
2.19	26.5	26.4	26.0	25.7	25.4	25.2	25.2
2.23	27.1	26.5	26.3	26.2	26.1	26.0	26.2
2.27	26.8	26.8	26.6	26.5	26.4	26.3	26.4
3.02	26.8	26.8	26.7	26.6	26.4	26.3	26.4
3.06	26.8	26.7	26.5	26.4	26.1	26.0	26.0
3.10	26.8	26.7	26.5	26.4	26.2	26.0	26.1
3.14	26.7	26.6	26.3	26.1	25.8	25.6	25.6
3.19	26.6	26.6	26.4	26.2	25.9	25.8	25.8
3.23	26.7	26.6	26.5	26.4	26.2	26.1	26.2
3.27	26.7	26.6	26.4	26.2	26.0	25.8	25.8
3.31	26.7	26.6	26.4	26.1	25.9	25.7	25.8
4.04	26.7	26.6	26.4	26.4	26.2	26.0	26.1
4.09	26.7	26.7	26.6	26.5	26.4	26.2	26.4
4.13	26.8	26.8	26.7	26.6	26.4	26.3	26.4
4.17	26.9	26.9	26.8	26.8	26.7	26.6	26.7
4.21	27.0	27.0	26.9	26.9	26.8	26.7	26.8
4.25	27.0	27.1	27.0	27.0	26.9	26.8	26.9
4.29	27.1	27.1	27.0	26.9	26.8	26.6	26.7
5.03	27.1	27.2	27.1	27.0	26.9	26.8	26.9
5.06	27.1	27.2	27.1	27.1	27.0	26.9	27.0
5.10	27.2	27.2	27.2	27.2	27.1	27.0	27.1
5.14	27.2	27.2	27.1	27.1	26.9	26.8	26.9
5.16	27.2	27.2	27.1	27.1	26.9	26.8	26.9
5.20	27.2	27.3	27.2	27.2	27.0	26.9	27.0
5.24	27.3	27.3	27.3	27.2	27.1	27.0	27.1
5.28	27.3	27.4	27.3	27.3	27.3	27.1	27.3
6.01	27.3	27.4	27.3	27.3	27.2	27.1	27.2
6.05	27.3	27.3	27.3	27.2	27.1	27.0	27.1
6.09	27.3	27.4	27.3	27.3	27.2	27.1	27.2

THERMISTOR	TH140	TH130	TH120	TH110	TH105	TH103	TH100
DATE	TEMPERATURES						
6.13	27.4	27.5	27.4	27.5	27.4	27.3	27.5
6.17	27.4	27.5	27.4	27.4	27.4	27.2	27.4
6.21	27.5	27.6	27.6	27.7	27.8	27.7	27.9
6.25	27.6	27.7	27.8	27.9	27.9	27.9	28.1
6.28	27.7	27.8	27.8	27.9	27.9	27.9	28.0
7.02	27.6	27.7	27.7	27.7	27.7	27.6	27.7
7.05	27.7	27.8	27.8	27.9	27.9	27.8	28.0
7.09	27.7	27.9	27.9	28.1	28.1	28.0	28.2
7.13	27.8	27.9	27.9	27.9	27.8	27.7	27.9
7.20	27.7	27.7	27.7	27.6	27.5	27.3	27.5
7.27	27.6	27.6	27.4	27.4	27.2	27.0	27.1

STRING #2 NO. OF THERMISTORS 3

THERMISTOR POSITION	TH230 2.50'	TH205 0.0'	TH200 -.50'
DATE	TEMPERATURES		
1.15	26.8	25.1	25.4
1.16	26.8	25.8	25.3
1.18	26.8	25.3	25.9
1.19	26.9	25.9	25.3
1.20	26.9	26.1	25.6
1.22	26.9	26.2	25.7
1.25	27.1	26.6	26.1
1.28	27.4	27.2	26.8
1.31	27.5	27.2	26.8
2.04	27.5	27.2	27.0
2.07	27.7	27.4	27.6
2.10	27.6	26.9	26.8
2.13	27.5	26.3	26.7
2.16	27.0	25.3	25.0
2.19	26.9	25.5	25.0
2.23	27.3	27.2	27.1
2.27	27.4	26.7	26.3
3.02	27.3	26.4	26.1
3.06	27.1	26.1	25.7
3.10	27.1	26.2	26.1
3.14	27.0	25.7	25.0
3.19	27.0	26.0	25.7
3.23	27.1	26.4	26.1
3.27	27.0	26.0	26.1
3.31	27.0	26.0	25.7
4.04	27.0	26.4	26.1
4.09	27.2	26.9	26.4
4.13	27.3	26.6	26.5
4.17	27.4	27.1	27.0
4.21	27.6	27.2	27.1
4.25	27.5	27.2	27.3
4.29	27.5	26.9	26.7
5.03	27.6	27.5	27.5
5.06	27.7	27.4	27.3
5.10	27.7	27.5	27.4
5.14	27.7	27.2	27.0
5.16	27.7	27.2	27.0
5.20	27.7	27.3	27.1
5.24	27.8	27.4	27.2
5.28	27.9	27.7	27.6
6.01	27.9	27.7	27.2
6.05	27.8	27.6	27.2
6.09	27.9	27.6	27.4

THERMISTOR	TH230	TH205	TH200
DATE	TEMPERATURE		
6.13	28.0	28.0	28.0
6.17	28.0	27.7	27.7
6.21	28.2	28.5	28.9
6.25	28.4	28.7	29.0
6.28	28.5	28.7	28.8
7.02	28.3	28.2	28.6
7.05	28.4	28.6	28.8
7.09	28.6	28.9	29.1
7.13	28.5	28.4	28.3
7.20	28.3	27.8	27.5
7.27	28.1	27.4	27.0

STRING #3 NO.OF THERMISTORS 3

THERMISTOR POSITION	TH330 3.0'	TH310 1.0'	TH300 0.0'
DATE	TEMPERATURES		
1.18	25.4	25.2	25.7
1.19	25.4	25.2	25.6
1.20	25.7	25.3	25.7
1.22	26.3	25.4	25.8
1.25	26.7	26.1	26.1
1.28	27.2	26.4	26.3
1.31	26.6	26.7	27.3
2.04	26.6	26.5	27.1
2.07	26.8	27.0	28.0
2.10	26.9	26.8	26.8
2.13	26.5	26.5	26.8
2.16	26.2	25.2	24.9
2.19	25.8	24.9	24.9
2.23	26.1	26.4	27.9
2.27	26.5	26.5	26.9
3.02	26.5	26.8	26.3
3.06	26.2	26.0	26.3
3.10	25.9	25.9	26.3
3.14	25.9	25.3	25.0
3.19	25.8	25.3	25.4
3.23	25.9	26.7	25.5
3.27	25.8	25.3	25.5
3.31	25.7	25.2	25.2
4.04	25.7	25.4	25.7
4.09	25.8	25.7	26.1
4.13	26.0	25.8	26.2
4.17	26.2	26.1	26.9
4.21	26.3	26.3	26.8
4.25	26.4	26.5	27.0
4.29	26.5	26.4	26.5
5.03	27.8	26.9	26.6
5.06	26.8	26.8	27.2
5.10	27.0	27.1	27.6
5.14	26.9	26.7	26.9
5.16	26.9	26.7	26.9
5.20	26.9	26.9	27.1
5.24	27.1	27.0	27.2
5.28	27.1	27.2	27.8
6.02	27.3	27.1	27.1
6.05	27.1	27.0	27.2
6.09	27.3	27.2	27.4
6.13	27.4	27.5	28.3

THERMISTOR	TH330	TH310	TH300
DATE	TEMPERATURES		
6.17	27.4	27.4	27.8
6.21	27.7	28.5	30.0
6.25	28.2	28.7	29.7
6.29	28.2	28.7	29.7
7.01	27.9	28.0	29.0
7.05	28.1	28.5	29.5
7.09	28.3	29.0	30.1
7.13	28.3	28.4	28.7
7.20	28.3	27.8	27.5
7.27	28.1	27.4	27.0

STRING #4 NO. OF THERMISTORS 2

THERMISTOR POSITION	TH420 2.0'	TH410 1.0'
DATE	TEMPERATURES	
1.18	24.4	24.8
1.19	24.4	24.8
1.20	24.3	24.8
1.22	24.4	24.8
1.25	25.0	24.7
1.28	25.2	24.9
1.31	25.3	25.0
2.04	25.4	25.2
2.07	25.6	25.4
2.10	25.5	25.2
2.13	25.2	24.6
2.16	24.3	23.3
2.19	24.2	23.6
2.23	24.6	24.2
2.27	25.0	24.6
3.02	24.5	24.9
3.06	24.9	24.5
3.10	24.8	24.3
3.14	24.7	24.1
3.19	24.8	24.5
3.23	24.9	25.1
3.27	25.0	24.7
3.31	25.4	24.6
4.04	25.1	24.9
4.08	25.4	25.3
4.13	25.3	25.3
4.17	25.7	25.7
4.21	25.8	25.7
4.25	25.9	25.9
4.29	25.9	25.7
5.03	25.7	25.4
5.06	25.7	25.4
5.10	25.6	25.3
5.14	25.6	25.2
5.16	25.6	25.2
5.20	25.6	25.3
5.24	25.6	25.3
5.28	25.7	25.4
6.02	25.6	25.3
6.05	25.6	25.3

THERMISTOR	1	0
DATE	TEMPERATURE	
6.09	25.7	25.5
6.13	25.8	25.5
6.17	25.8	25.6
6.21	25.9	25.6
6.25	25.9	25.7
6.28	25.9	25.7
7.02	25.6	25.9
7.05	25.9	25.6
7.09	25.9	25.6
7.13	25.9	25.6
7.20	25.8	25.5
7.27	25.8	25.5

STRING #5 NO. OF THERMISTORS 3

THERMISTOR POSITION	TH530 3.0'	TH515 1.5'	TH500 0.0'
DATE	TEMPERATURE		
1.22	24.2	23.7	23.8
1.25	24.3	24.1	24.2
1.28	24.5	24.4	24.7
1.31	24.7	24.6	24.8
2.04	24.8	24.6	25.0
2.07	25.0	25.0	25.5
2.10	25.1	25.0	25.1
2.13	25.0	24.5	24.0
2.16	24.2	23.1	22.4
2.19	23.8	22.9	22.7
2.23	23.9	23.5	25.3
2.27	24.1	24.4	24.3
3.02	24.3	24.0	23.9
3.06	24.2	23.7	23.7
3.10	24.2	23.7	23.7
3.14	24.0	23.4	23.0
3.19	24.1	23.8	24.0
3.23	24.3	24.2	24.8
3.27	24.4	24.1	24.2
3.31	24.4	23.9	24.0
4.04	24.4	24.1	24.5
4.09	24.6	24.5	24.9
4.13	24.8	24.6	25.0
4.17	25.1	25.1	25.9
4.21	25.2	25.2	25.6
4.25	25.4	25.4	26.0
4.29	25.3	25.1	25.0
5.03	25.3	25.0	25.0
5.06	25.3	25.1	25.0
5.10	25.2	24.9	24.9
5.14	24.8	24.8	24.8
5.16	25.1	24.7	24.8
5.20	25.1	24.8	24.9
5.24	25.1	24.8	25.3
5.28	25.2	25.3	25.1
6.02	25.2	24.8	24.9
6.05	25.1	24.8	24.8
6.09	25.1	24.9	25.4
6.13	25.2	25.0	25.2

THERMISTOR	TH530	TH515	TH500
DATE	TEMPERATURE		
6.17	25.3	25.3	25.4
6.21	25.4	25.2	25.5
6.25	25.5	25.2	25.5
6.28	25.5	25.2	25.4
7.02	25.5	25.1	25.2
7.05	25.4	25.2	25.3
7.09	25.5	25.2	25.4
7.14	25.5	25.2	25.2
7.20	25.3	25.0	25.0
7.27	25.3	25.3	24.9

STRING #6 NO. OF THERMISTORS 5

THERMISTOR POSITION	TH675 7.5'	TH655 5.5'	TH645 4.5'	TH625 2.5'	TH600 0.0'
DATE	TEMPERATURE				
1.15	26.3	26.6	26.5	25.9	25.2
1.16	26.2	26.6	26.4	25.9	25.9
1.18	26.2	26.5	26.4	26.0	25.9
1.19	26.1	26.5	26.4	26.1	26.1
1.20	26.1	26.5	26.4	26.2	26.3
1.22	26.1	26.6	26.5	26.3	26.5
1.25	26.2	26.7	26.6	26.6	26.5
1.28	26.2	26.8	26.8	26.9	27.1
1.31	26.3	27.0	27.0	27.2	27.0
2.04	26.4	27.1	27.1	27.2	27.1
2.07	26.5	27.2	27.2	27.5	27.4
2.10	26.5	27.3	27.3	27.5	27.0
2.13	26.6	27.3	27.3	27.2	26.6
2.16	26.6	27.1	27.0	26.3	25.2
2.19	26.5	26.8	26.6	25.9	24.9
2.23	26.3	26.7	26.7	26.7	27.4
2.27	26.3	27.0	26.9	27.0	26.9
3.02	26.4	27.0	27.0	27.0	26.8
3.06	26.4	27.0	26.9	26.8	26.4
3.10	26.4	26.9	26.8	26.7	26.5
3.14	26.3	26.8	26.6	26.2	25.4
3.19	26.2	26.6	26.5	26.2	25.5
3.23	26.2	26.6	26.5	26.3	25.8
3.27	26.2	26.6	26.5	26.2	25.5
3.31	26.1	26.6	26.5	26.1	25.4
4.04	26.1	26.6	26.4	26.2	25.7
4.09	26.1	26.6	26.6	26.5	26.0
4.13	26.2	26.7	26.7	26.6	26.2
4.17	26.2	26.8	26.8	26.8	27.0
4.21	26.3	26.9	26.9	27.0	26.7
4.25	26.4	27.1	27.1	27.1	26.8
4.29	26.5	27.1	27.1	27.1	26.8
5.03	26.6	27.3	27.3	27.6	27.8
5.06	26.6	27.3	27.4	27.6	27.4
5.10	26.7	27.5	27.5	27.8	27.6
5.14	26.8	27.5	27.5	27.5	27.0
5.16	26.8	27.5	27.5	27.5	26.9
5.20	26.8	27.5	27.5	27.6	27.2
5.24	26.8	27.6	27.6	27.8	27.3
5.28	26.9	27.6	27.7	27.9	27.7

THERMISTOR	TH675	TH655	TH645	TH625	TH600
DATE	TEMPERATURE				
6.01	27.0	27.7	27.7	27.8	27.3
6.05	27.0	27.7	27.7	27.7	27.2
6.09	27.0	27.7	27.8	27.9	27.5
6.13	27.1	27.8	27.9	28.2	28.3
6.17	27.1	27.9	27.9	28.0	27.8
6.21	27.2	27.9	28.1	28.6	29.8
6.25	27.0	28.1	28.3	29.0	29.5
6.28	27.4	28.3	28.5	29.0	29.4
7.02	27.5	28.3	28.4	28.5	28.6
7.05	27.5	28.4	28.5	28.9	29.3
7.09	27.5	28.5	28.6	29.2	29.7
7.13	27.6	28.6	28.7	28.9	28.6
7.20	27.6	28.4	28.5	28.9	29.3
7.27	27.5	28.1	28.0	27.8	27.3

STRING# 7 NO. OF THERMISTORS 5

THERMISTOR POSITION	TH790 9.0'	TH760 6.0'	TH750 5.0'	TH720 2.0'	TH700 0.0'
DATE	TEMPERATURE (DEGREES F.)				
1.15	26.9	26.1	25.5	25.0	26.3
1.16	26.9	25.9	25.8	26.3	26.6
1.18	26.8	25.9	25.9	26.3	26.0
1.19	26.8	25.9	26.2	26.3	26.7
1.20	26.8	25.9	26.2	26.4	27.3
1.22	26.8	26.0	26.2	26.4	27.5
1.25	26.8	26.0	26.2	26.5	26.5
1.28	26.8	26.0	26.4	26.5	27.2
1.31	26.8	26.1	26.6	26.6	26.8
2.04	26.9	26.2	26.6	26.7	28.4
2.07	26.9	26.3	26.8	26.8	28.0
2.10	26.9	26.4	26.9	26.8	27.1
2.13	27.0	26.4	26.9	26.5	26.4
2.16	27.0	26.3	26.7	25.7	24.9
2.19	27.0	26.1	26.4	25.4	24.7
2.23	26.0	25.9	26.2	25.9	26.6
2.27	26.8	26.0	26.4	26.1	26.0
3.02	26.8	26.0	26.4	26.1	25.9
3.06	26.8	26.0	26.4	25.9	25.6
3.10	26.8	26.0	26.3	25.9	25.7
3.14	26.8	25.9	26.0	25.6	25.3
3.19	26.7	25.8	26.4	25.7	25.4
3.23	26.7	25.8	26.2	25.9	25.9
3.27	26.7	25.8	26.2	25.8	25.5
3.31	26.7	25.8	26.2	25.7	25.5
4.04	26.7	25.8	26.2	25.8	25.8
4.09	26.7	25.9	26.3	26.1	26.1
4.13	26.7	26.0	26.4	26.2	26.3
4.17	26.8	26.1	26.6	26.5	26.7
4.21	26.8	26.2	26.7	26.7	26.8
4.25	26.9	26.3	26.8	26.8	27.0
4.29	27.0	26.4	26.9	26.8	26.8
5.03	27.0	26.5	27.0	27.2	27.5
5.06	27.1	26.6	27.1	27.2	27.4
5.10	27.1	26.7	27.2	27.5	27.7
5.14	27.2	26.8	27.3	27.2	27.0
5.16	27.2	26.8	27.3	27.1	26.9
5.20	27.3	26.7	27.2	27.2	27.2
5.24	27.3	26.8	27.3	27.4	27.4
5.28	27.3	26.9	27.4	27.6	27.8
6.01	27.4	27.4	27.4	27.5	27.7
6.05	27.4	27.0	27.5	27.4	27.3
6.09	27.0	27.7	27.9	27.5	27.8
6.13	27.5	27.0	27.5	27.5	27.8

THERMISTOR	TH790	TH760	TH750	TH720	TH700
DATE	TEMPERATURE (DEGREES F.)				
6.17	27.5	27.0	27.6	27.6	27.6
6.21	27.5	27.1	27.6	27.9	28.7
6.25	27.6	27.2	27.8	28.6	28.7
6.28	27.7	27.4	28.0	28.4	28.7
7.02	27.8	27.4	28.0	28.0	28.3
7.05	27.8	27.4	28.0	28.2	28.6
7.09	27.8	27.5	28.0	28.4	28.7
7.13	27.9	27.6	28.0	28.3	28.2
7.20	27.9	27.5	28.0	27.8	27.6
7.27	27.9	27.3	27.4	27.4	27.2

APPENDIX B

Summary of Convergence Measurements

CONVERGENCE MEASUREMENTS

STATION	1	2	3	4
DATE	CUMULATIVE CONVERGENCE			
1.20	.000	.000	.000	.000
1.22	.002	.004	.003	.003
1.25	.007	.003	.007	.002
1.28	.003	.016	.003	.008
1.31	.015	.013	.008	.010
2.04	.012	.014	.009	.010
2.07	.022	.022	.016	.016
2.10	.036	.025	.018	.020
2.13	.022	.025	.017	.020
2.16	.029	.027	.018	.023
2.19	.029	.027	.018	.023
2.23	.036	.037	.015	.041
2.27	.035	.038	.028	.038
3.02	.035	.043	.028	.042
3.06	.057	.043	.048	.064
3.10	.062	.048	.052	.080
3.14	.067	.050	.053	.080
3.19	.074	.054	.058	.084
3.23	.074	.057	.063	.086
3.27	.075	.057	.077	.084
3.31	.075	.057	.077	.084
4.04	.077	.060	.075	.087
4.09	.079	.064	.080	.088
4.13	.082	.065	.085	.088
4.17	.089	.074	.089	.100
4.21	.089	.074	.095	.100
4.25	.093	.087	.095	.103
4.29	.093	.087	.097	.106
5.03	.099	.097	.108	.111
5.06	.100	.097	.111	.111
5.10	.105	.099	.118	.111
5.14	.110	.106	.122	.112
5.16	.112	.101	.122	.120
5.20	.117	.107	.123	.122
5.24	.119	.109	.129	.124
5.28	.121	.120	.140	.138
6.01	.127	.120	.142	.145
6.05	.137	.127	.146	.147
6.09	.141	.130	.154	.150
6.13	.148	.137	.162	.155

STATION	1	2	3	4
DATE	CUMULATIVE CONVERGENCE			
6.17	.153	.148	.163	.162
6.21	.155	.152	.177	.169
6.25	.158	.166	.177	.176
6.28	.164	.171	.182	.191
7.02	.164	.185	.195	.199
7.05	.174	.193	.201	***
7.09	.194	.209	.202	****
7.13	.197	.210	.217	****
7.20	.209	.225	.220	****
7.27	.219	.239	.230	****

CONVERGENCE MEASUREMENTS

STATION	5	6	7	8
DATE	CUMULATIVE CONVERGENCE			
1.20	.000	.000	.000	.000
1.22	.023	.003	.000	.004
1.25	.023	.003	.026	.019
1.28	.021	.003	.017	.010
1.31	.029	.016	.023	.007
2.04	.027	.018	.019	.022
2.07	.031	.028	.017	.022
2.10	.030	.028	.017	.026
2.13	.032	.028	.013	.026
2.16	.032	.024	.008	.032
2.19	.032	.024	.023	.036
2.23	.039	.038	.025	.036
2.27	.037	.022	.020	.036
3.02	.038	.032	.022	.043
3.06	.058	.054	.051	.064
3.10	.064	.060	.052	.064
3.14	.066	.060	.052	.064
3.19	.071	.060	.052	.070
3.23	.072	.060	.052	.071
3.27	.072	.060	.052	.072
3.31	.076	.061	.053	.072
4.04	.076	.068	.058	.078
4.09	.079	.072	.063	.082
4.13	.083	.077	.067	.083
4.17	.088	.082	.069	.093
4.21	.090	.086	.072	.099
4.25	.097	.092	.072	.104
4.29	.099	.093	.075	.104
5.03	.101	.093	.079	.105
5.06	.105	.096	.085	.120
5.10	.105	.096	.085	.120
5.14	.106	.101	.085	.120
5.16	.106	.101	.085	.124
5.20	.112	.114	.091	.127
5.24	.114	.115	.091	.132
5.28	.117	.115	.095	.139
6.02	.124	.123	.101	.141
6.05	.130	.130	.101	.141
6.09	.134	.131	.103	.141
6.13	.149	.135	.106	.151

STATION	5	6	7	8
DATE	CUMULATIVE CONVERGENCE			
6.17	.153	.137	.118	.157
6.21	.155	.140	.118	.160
6.25	.157	.141	.118	.160
6.28	.171	.146	.122	.161
7.02	****	.146	.122	.161
7.05	.190	.153	.125	.162
7.09	****	.153	.126	.166
7.13	.215	.157	.126	.167
7.20	****	.160	****	.171
7.27	****	.171	****	.173

APPENDIX C

Two-way Randomized Block Design and Analysis

In order to identify the influence of geometry and overburden, a random block analysis was used. Two independent factors, temperature of frozen ground at 1 ft. and locality of convergence stations, were used as column- and row-factor. The recorded creep rate was the observation. The randomized block for this case is listed in Table IV.

The missing data technique for the two way table was applied to estimate the probable missing data at stations C5 and C4 at 27.3°F. The following equations were used:

$$(m-1)(n-1)x = mR1 + nC1 - S - y$$

$$(m-1)\ (n-1)\ y = mR2 + nC2 - S - X$$

where

- m is the number of rows
- n is the number of columns
- R1 is the total known observation of row containing X.
- R2 is the total of known observation of row containing y.
- C1 is the total of known observation of column containing X.
- C2 is the total of known observation of column containing y.
- S is the total of all known results.

Table IV. Summary of creep and ground temperature for USBM gravel room

	25.4	25.7	26.1	26.5	26.7	26.9	27.1	27.3	27.9	28.5	
C5	5.4	4.6	11.3	3.6	6.1	6.4	13.3	X	15.3	29.4	95.4 + X
C4	3.1	3.1	9.4	12.9	6.4	9.3	17.3	y	24	16.3	101.8 + Y
C1	3.1	6.2	8.8	9.3	10.0	10	14.7	14.3	10	15.6	102
C2	5.4	6.2	13.1	5.0	9.7	7.1	15.3	20	24	21.7	127.5
C3	2.3	18.5	9.4	7.9	11.9	7.9	16.7	14.3	15.3	17.2	121.4
	19.3	38.6	52	38.7	44.1	40.7	77.3	X + Y + 48.6	88.6	100.2	548.1 + x + y

The estimated creep rate was 11.2×10^{-4} in./day at station C5 and was 12.1×10^{-4} in./day at station C4 (Table III). With these two calculated values the randomized block was completed and shown in Table V. Step by step, the corrections for the mean (CM), total sum of squares (TSS), sum of squares between columns (SSC), sum of squares between rows (SSR), and sum of squares due to error (SSE) were calculated. The analysis of variance is listed in the Table VI.

Table V. Two-way randomized block design

	25.4	25.7	26.1	26.5	26.7	26.9	27.1	27.3	27.9	28.5	
C5	5.4	4.6	11.3	3.6	6.1	6.4	13.3	11.20	15.3	29.4	106.6
C4	3.1	3.1	9.4	12.9	6.4	9.3	17.3	12.10	24	16.3	113.9
C1	3.1	6.2	8.8	9.3	10.0	10	14.7	14.3	10	15.6	102
C2	5.4	6.2	13.1	5.0	9.7	7.1	15.3	20	24	21.7	127.5
C3	2.3	18.5	9.4	7.9	11.9	7.9	16.7	14.3	15.3	17.2	121.4
	19.3	38.6	52	38.7	44.1	40.7	77.3	17.1	88.6	100.2	571.4

Table VI. ANOVA table for two-way analysis

Source of Variation	Degree of Freedom	Sum of Squares	Mean Square	F-Value Calculated	F-Value $\alpha = 0.05$	F-Value $\alpha = 0.01$
Temperature	9	1210.11	134.46	8.7	2.16	2.96
Locality	4	43.54	10.89	0.70	2.64	3.91
Error	36	556.39	15.46			